Chapter 7
The Higgs Mechanism and the Standard Model of Particle Physics

The basic interactions affecting matter at the particle physics level are electromagnetism, strong interaction, and weak interaction. They can be unified by a Lagrangian displaying gauge invariance with respect to the $\mathrm{SU}(3) \otimes \mathrm{SU}(2) \otimes \mathrm{U}(1)$ *local symmetry group; this unification is called the standard model of particle physics. Within the standard model, an elegant mechanism, called the Higgs mechanism, accounts for the appearance of masses of particles and of some of the gauge bosons. The standard model is very successful, since it brilliantly passed extremely accurate precision tests and several predictions have been confirmed—in particular, the Higgs particle has been recently discovered in the predicted mass range. However, it can hardly be thought as the final theory of nature: some physics beyond the standard model must be discovered to account for gravitation and to explain the energy budget of the Universe.*

In the previous chapter, we have characterized three of the four known interactions: the electromagnetic, strong interaction, and weak interaction.

We have presented an elegant mechanism for deriving the existence of gauge bosons from a local symmetry group. We have carried out in detail the calculations related to the electromagnetic theory, showing that the electromagnetic field naturally appears from imposing a local U(1) gauge invariance. However, a constraint imposed by this procedure is that the carriers of the interactions are massless. If we would like to give mass to the photons, we would violate the gauge symmetry:

$$\frac{1}{2}M_A^2 A_\mu A^\mu \rightarrow \frac{1}{2}M_A^2 (A_\mu - \frac{1}{e}\partial_\mu \alpha)\left(A^\mu - \frac{1}{e}\partial^\mu \alpha\right) \neq \frac{1}{2}M_A^2 A_\mu A^\mu \tag{7.1}$$

A. De Angelis and M. Pimenta, *Introduction to Particle and Astroparticle Physics*, Undergraduate Lecture Notes in Physics,
https://doi.org/10.1007/978-3-319-78181-5_7

if $M_A \neq 0$. This is acceptable in this particular case, being the carriers of electromagnetic interaction identified with the massless photons, but not in general.

A similar situation applies to the theory of strong interactions, QCD. The symmetry with respect to rotation in color space, SU(3), entails the appearance of eight massless quanta of the field, the gluons, which successfully model the experimental observations.

The representation of the weak interaction has been less satisfactory. We have a SU(2) symmetry there, a kind of isospin, but the carriers of the force must be massive to explain the weakness and the short range of the interaction—indeed they are identified with the known $W^{\pm}$ and Z particles, with a mass of the order of 100 GeV. But we do not have a mechanism for explaining the existence of massive gauge particles, yet. Another problem is that, as we shall see, incorporating the fermion masses in the Lagrangian by brute force via a Dirac mass term $m\bar{\psi}\psi$ would violate the symmetry related to the weak interaction.

Is there a way to generate the gauge boson and the fermion masses without violating gauge invariance? The answer is given by the so-called Higgs mechanism, proposed in the 1960s. This mechanism is one of the biggest successes of fundamental physics and requires the presence of a new particle; the Higgs boson, responsible for the masses of particles. This particle has been found experimentally in 2012 after 50 years of searches—consistent with the standard model parameters measured with high accuracy at LEP.

The Higgs mechanism allowed to formulate a quantum field theory—relativistically covariant—that explains all currently observed phenomena at the scale of elementary particles: the standard model of particle physics (in short "standard model," also abbreviated as SM). The SM includes all the known elementary particles and the three interactions relevant at the particle scale: the electromagnetic interaction, the strong interaction, and the weak interaction. It does not include gravitation, which, for now, cannot be described as a quantum theory. It is a $\mathrm{SU}(3) \otimes \mathrm{SU}(2) \otimes \mathrm{U}(1)$ symmetrical model.

The SM is built from two distinct interactions affecting twelve fundamental particles (quarks and leptons) and their antiparticles: the electroweak interaction, coming from the unification of the weak force and electromagnetism (QED), and the strong interaction explained by QCD. These interactions are explained by the exchange of gauge bosons (the vectors of these interactions) between elementary fermions.

All our knowledge about fundamental particles and interactions, which we have described in the previous chapters, can be summarized in the following table.

Some remarks about the table:

- Elementary particles are found to be all spin one-half particles. They are divided into quarks, which are sensitive to the strong interaction, and "leptons" which have no strong interactions. No reason is known neither for their number, nor for their properties, such as their quantum numbers.

TABLE OF ELEMENTARY PARTICLES		
QUANTA OF RADIATION		
Strong Interactions		Eight gluons
Electromagnetic Interactions		Photon (γ)
Weak Interactions		Bosons $W^{\pm}$, Z
Gravitational Interactions		Graviton (?)
MATTER PARTICLES		
	Leptons	Quarks
1st Family	$(\nu_e\ ,\ e^-)$	$(u\ ,\ d)$
2nd Family	$(\nu_\mu\ ,\ \mu^-)$	$(c\ ,\ s)$
3rd Family	$(\nu_\tau\ ,\ \tau^-)$	$(t\ ,\ b)$
HIGGS BOSON		

- Quarks and leptons can be organized into three distinct groups or "families." No deep explanation is known.
- Each quark species, called "flavor," appears under three charges, called "colors."
- Quarks and gluons do not appear as free particles. They are confined in bound states, the hadrons.

Let us see which mechanism can explain the mass of gauge bosons.

7.1 The Higgs Mechanism and the Origin of Mass

The principle of local gauge invariance works beautifully for electromagnetic interactions. Veltman and 't Hooft[1] proved in the early 1970s that gauge theories are renormalizable. But gauge fields appear to predict the existence of massless gauge bosons, while we know in nature that weak interaction is mediated by heavy vectors $W^{\pm}$ and Z.

How to introduce mass in a gauge theory? We have seen that a quadratic term $\mu^2 A^2$ in the gauge boson field spoils the gauge symmetry; gauge theories seem, at face value, to account only for massless gauge particles.

The idea to solve this problem came from fields different from particle physics, and it is related to spontaneous symmetry breaking.

[1] Martinus Veltman (1931) is a Dutch physicist. He supervised the Ph.D. thesis of Gerardus't Hooft (1946), and during the thesis work, in 1971, they demonstrated that gauge theories were renormalizable. For this achievement, they shared the Nobel Prize for Physics in 1999.

7.1.1 Spontaneous Symmetry Breaking

Spontaneous symmetry breaking (SSB) was introduced into particle physics in 1964 by Englert and Brout, and independently by Higgs.[2] Higgs was the first to mention explicitly the appearance of a massive scalar particle associated with the curvature of the effective potential that determines the SSB; the mechanism is commonly called the Higgs mechanism, and the particle is called the Higgs boson.

Let us see how SSB can create in the Lagrangian a mass term quadratic in the field. We shall concentrate on a scalar theory, but the extension to a vector theory does not add conceptually.

The idea is that the system has at least two phases:

- The unbroken phase: the physical states are invariant with respect to all symmetry groups with respect to which the Lagrangian displays invariance. In a local gauge theory, massless vector gauge bosons appear.
- The spontaneously broken phase: below a certain energy, a phase transition might occur. The system reaches a state of minimum energy (a "vacuum") in which part of the symmetry is hidden from the spectrum. For a gauge theory, we shall see that some of the gauge bosons become massive and appear as physical states.

Infinitesimal fluctuations of a system which is crossing a critical point can decide on the system's fate, by determining which branch among the possible ones is taken. Such fluctuations arise naturally in quantum physics, where the vacuum is just the point of minimal energy and not a point of zero energy.

It is this kind of phase transition that we want to study now.

7.1.2 An Example from Classical Mechanics

Consider the bottom of an empty wine bottle (Fig. 7.1). If a ball is put at the peak of the dome, the system is symmetrical with respect to rotating the bottle (the potential is rotationally symmetrical with respect to the vertical axis). But below a certain energy (height), the ball will spontaneously break this symmetry and move into a point of lowest energy. The bottle continues to have symmetry, but the system no longer does.

---

[2] Peter Higgs (Newcastle, UK, 1929) has been taught at home having missed some early schooling. He moved to city of London School and then to King's College also in London, at the age of 17 years, where he graduated in molecular physics in 1954. In 1980, he was assigned the chair of Theoretical Physics at Edinburgh. He shared the 2013 Nobel Prize in physics with François Englert "for the theoretical discovery of a mechanism that contributes to our understanding of the origin of mass of subatomic particles, and which recently was confirmed through the discovery of the predicted fundamental particle." François Englert (1932) is a Belgian physicist; he is a Holocaust survivor. After graduating in 1959 at Université Libre de Bruxelles, he was nominated full professor at the same University in 1980, where he worked with Brout. Brout had died in 2011 and could not be awarded the Nobel Prize.

Fig. 7.1 The potential described by the shape of the *bottom* of an empty bottle. Such a potential is frequently called "mexican hat" or "cul-de-bouteille," depending on the cultural background of the author

In this case, what happens to the original symmetry of the equations? It still exists in the sense that if a symmetry transformation is applied (in this case a rotation around the vertical axis) to the asymmetric solution, another asymmetric solution which is degenerate with the first one is obtained. The symmetry has been "spontaneously broken." A spontaneously broken symmetry has the characteristics, evident in the previous example, that a critical point, i.e., a critical value of some external quantity which can vary (in this case, the height from the bottom, which corresponds to the energy), exists, which determines whether symmetry breaking will occur. Beyond this critical point, frequently called a "false vacuum," the symmetric solution becomes unstable, and the ground state becomes asymmetric—and degenerate.

Spontaneous symmetry breaking appears in many phenomena, for example, in the orientation of domains in a ferromagnet, or in the bending of a rod pushed at its extremes (beyond a certain pressure, the rod must bend in a direction, but all directions are equivalent).

We move to applications to field theory, now.

7.1.3 Application to Field Theory: Massless Fields Acquire Mass

We have seen that a Lagrangian density

$$\mathcal{L}_0 = (\partial^\mu \phi^*)(\partial_\mu \phi) - M^2 \phi^* \phi \tag{7.2}$$

with M^2 real and positive and ϕ a complex scalar field

$$\phi(x) = \frac{1}{\sqrt{2}} (\phi_1(x) + i\phi_2(x))$$

describes a free scalar particle of mass M.

Let us now consider a complex scalar field whose dynamics is described by the Lagrangian density:

$$\mathcal{L}_1 = (\partial^\mu \phi^*)(\partial_\mu \phi) - \mu^2 \phi^* \phi - \lambda(\phi^* \phi)^2 \tag{7.3}$$

with $\lambda > 0$; let μ^2 be just a (real) parameter now.

The Lagrangians (7.2) and (7.3) are invariant under the group U(1) describing the global symmetry of rotation:

$$\phi(x) \rightarrow e^{i\theta} \phi(x) \,. \tag{7.4}$$

Let us try now to find the points of stability for the system (7.3). The potential associated to the Lagrangian is

$$V(\phi) = \mu^2 \phi^* \phi + \lambda(\phi^* \phi)^2 \tag{7.5}$$

and, as a function of the component fields,

$$V(\phi) = \frac{1}{2}\mu^2(\phi_1^2 + \phi_2^2) + \frac{1}{4}\lambda(\phi_1^2 + \phi_2^2)^2 \,. \tag{7.6}$$

The position of the minimum depends on the sign of μ^2:

- for $\mu^2 > 0$, the minimum is at $\phi = 0$;
- for $\mu^2 < 0$, there is a circle of minima at the complex ϕ-plane with radius v

$$v = (-\mu^2/\lambda)^{1/2}$$

(Fig. 7.2). Any point on the circle corresponds to a spontaneous breaking of the symmetry of (7.4). Spontaneous symmetry breaking occurs, if the kinetic energy is smaller than the potential corresponding to the height of the dome. We call v the vacuum expectation value: $|\phi| = v$ is the new vacuum for the system, and the argument, i.e., the angle in the complex plane, can be whatever. The actual minimum is not symmetrical, although the Lagrangian is.

Let us assume, for simplicity, that the actual minimum chosen by the system is at argument 0 (ϕ is real); this assumption does not affect generality. We now define a new coordinate system in which a coordinate σ goes along ϕ_1 and a coordinate ξ is perpendicular to it (Fig. 7.3). Notice that the coordinate ξ does not have influence on the potential, since the latter is constant along the circumference. We examine the Lagrangian in the vicinity of the minimum. Choosing an appropriate scaling for ξ and σ, one can write

$$\phi = \frac{1}{\sqrt{2}}[(v + \sigma) + i\xi] \simeq \frac{1}{\sqrt{2}}(v + \sigma)e^{i\xi/v}$$

and thus

$$\partial_\mu \phi = \frac{i}{v}\partial_\mu \xi \phi + \frac{1}{\sqrt{2}} e^{i\xi/v} \partial_\mu \sigma \,.$$

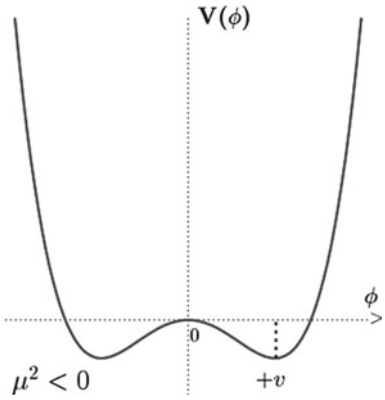

Fig. 7.2 The potential $V(\phi)$ with $\mu^2 < 0$ (cut on a plane containing the V axis)

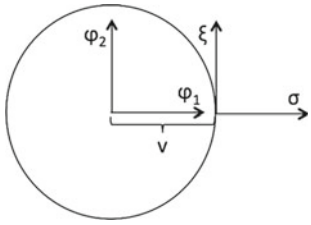

Fig. 7.3 Definition of the new fields σ and ξ

Hence, taking as zero the point of minimum,

$$\mathcal{L}_1 = \frac{1}{2}\partial_\mu\sigma\,\partial^\mu\sigma + \frac{1}{2}\partial_\mu\xi\,\partial^\mu\xi - \frac{1}{2}(-2\mu^2)\sigma^2 + \text{const.} + \mathcal{O}(3)\,. \tag{7.7}$$

The σ^2 term is a mass term, and thus the Lagrangian (7.7) describes a scalar field of mass $m_\sigma^2 = -2\mu^2 = 2\lambda v^2$.

Since there are now nonzero cubic terms in σ, the reflexion symmetry is broken by the ground state: after choosing the actual vacuum, the ground state does not show all the symmetry of the initial Lagrangian (7.3). But a U(1) symmetry operator still exists, which turns one vacuum state into another one along the circumference.

Note that the initial field ϕ had two degrees of freedom. One cannot create or cancel degrees of freedom; in the new system, one degree of freedom is taken by the field σ, while the second is now absorbed by the massless field ξ, which moves the potential along the "cul de bouteille." The appearance of massless particles is an aspect of the *Goldstone theorem,* which we shall not demonstrate here. The Goldstone theorem states that if a Lagrangian is invariant under a group of transformations $\mathcal{G}$ with n generators, and if there is a spontaneous symmetry breaking such that the new vacuum is invariant only under a group of transformations $\mathcal{G}' \subset \mathcal{G}$ with $m < n$ generators, then a number $(n - m)$ of massless scalar fields appear. These are called Goldstone bosons.

In the previous example, the Lagrangian had a U(1) symmetry (one generator). After the SSB, the system had no symmetry. One Goldstone field ξ appeared.

7.1.4 From SSB to the Higgs Mechanism: Gauge Symmetries and the Mass of Gauge Bosons

We have seen that spontaneous symmetry breaking can give a mass to a field otherwise massless, and as a consequence some additional massless fields appear—the Goldstone fields.

In this section, we want to study the consequences of spontaneous symmetry breaking in the presence of a local gauge symmetry, as seen from the case $\mu^2 < 0$ in the potential (7.5). We shall see that (some of the) gauge bosons will become massive, and one or more additional massive scalar field(s) will appear—the Higgs field(s). The Goldstone bosons will disappear as an effect of the gauge invariance: this is called the Higgs mechanism.

We consider the case of a local U(1) symmetry: a complex scalar field coupled to itself and to an electromagnetic field A_μ

$$\mathcal{L} = -\frac{1}{4} F_{\mu\nu} F^{\mu\nu} + (D_\mu \phi)^* (D^\mu \phi) - \mu^2 \phi^* \phi - \lambda \, (\phi^* \phi)^2 \tag{7.8}$$

with the covariant derivative $D_\mu = \partial_\mu + ieA_\mu$. If $\mu^2 > 0$, this Lagrangian is associated to electrodynamics between scalar particles, and it is invariant with respect to local gauge transformations

$$\begin{aligned} \phi(x) &\to \phi'(x) = e^{i\epsilon(x)} \, \phi(x) \\ A_\mu(x) &\to A'_\mu(x) = A_\mu(x) - \frac{1}{e} \, \partial_\mu \epsilon(x) \, . \end{aligned}$$

If $\mu^2 < 0$, we shall have spontaneous symmetry breaking. The ground state will be

$$\langle \phi \rangle = v = \sqrt{-\frac{\mu^2}{\lambda}} > 0 \, ; \tag{7.9}$$

and as in the previous section, we parametrize the field ϕ starting from the vacuum as

$$\phi(x) = \frac{1}{\sqrt{2}} (v + \sigma(x)) e^{i\xi(x)/v} \, . \tag{7.10}$$

We have seen in the previous section that the field $\xi(x)$ was massless and associated to the displacement between the degenerate ground states. But here the ground states are equivalent because of the gauge symmetry. Let us examine the consequences of this. We can rewrite Eq. 7.8 as

$$\mathcal{L} = -\frac{1}{4} F_{\mu\nu}F^{\mu\nu} + \frac{1}{2}\,\partial_\mu\sigma\,\partial^\mu\sigma + \frac{1}{2}\,\partial_\mu\xi\,\partial^\mu\xi + \frac{1}{2}e^2v^2A_\mu A^\mu - veA_\mu\partial^\mu\xi + \mu^2\sigma^2 + \mathcal{O}(3)\,. \tag{7.11}$$

Thus the σ field acquires a mass $m_\sigma^2 = -2\mu^2$; there are in addition mixed terms between A_μ and ξ. Let us make a gauge transformation

$$\epsilon(x) = -\frac{\xi(x)}{v}\,; \tag{7.12}$$

thus

$$\phi(x) \to \phi'(x) = e^{-i\xi(x)/v}\phi(x) = \frac{1}{\sqrt{2}}(v + \sigma(x)) \tag{7.13}$$

$$A_\mu(x) \to A'_\mu(x) + \frac{1}{ev}\partial_\mu\xi \tag{7.14}$$

and since the Lagrangian is invariant for this transformation, we must have

$$\begin{aligned}\mathcal{L}(\phi, A_\mu) &= \mathcal{L}(\phi', A'_\mu)\\ &= \frac{1}{2}\left[\left(\partial_\mu - ieA'_\mu\right)(v+\sigma)\right]\left[\left(\partial^\mu + ieA'^\mu\right)(v+\sigma)\right]\\ &\quad - \frac{1}{2}\,\mu^2\,(v+\sigma)^2 - \frac{1}{4}\,\lambda\,(v+\sigma)^4 - \frac{1}{4}\,F'_{\mu\nu}F'^{\mu\nu}\,.\end{aligned} \tag{7.15}$$

The Lagrangian in Eq. 7.15 can be also written as

$$\mathcal{L} = -\frac{1}{4}\,F'_{\mu\nu}F'^{\mu\nu} + \frac{1}{2}\,\partial_\mu\sigma\,\partial^\mu\sigma + \frac{1}{2}\,e^2v^2A'_\mu A'^\mu - \lambda v^2\sigma^2 + \mathcal{O}(3)\,, \tag{7.16}$$

and now it is clear that both σ and A_μ have acquired mass:

$$m_\sigma = \sqrt{2\lambda v^2} = \sqrt{-2\mu^2} \tag{7.17}$$

$$m_A = ev\,. \tag{7.18}$$

Notice that the field ξ is disappeared. This is called the *Higgs mechanism*; the massive (scalar) σ field is called the Higgs field. In a gauge theory, the Higgs field "eats" the Goldstone field.

Notice that the number of degrees of freedom of the theory did not change: now the gauge field A_μ is massive (three degrees of freedom), and the field σ has one degree of freedom (a total of four degrees of freedom). Before the SSB, the field had two degrees of freedom, and the massless gauge field an additional two—again, a total of four.

The exercise we just did is not appropriate to model electromagnetism—after all, the photon A_μ is massless to the best of our knowledge. However, it shows completely the technique associated to the Higgs mechanism.

We shall now apply this mechanism to explain the masses of the vectors of the weak interaction, the Z, and the $W^\pm$; but first, let us find the most appropriate description for the weak interaction, which is naturally linked to the electromagnetic one.

7.2 Electroweak Unification

The weak and electromagnetic interactions, although different, have some common properties which can be exploited for a more satisfactory—and "economical" description.

Let us start from an example, taken from experimental data. The $\Sigma^+(1189)$ baryon, a uus state, decays into $p\pi^0$ via a strangeness-changing weak decay (the basic transition at the quark level being $s \to ud\bar{u}$), and it has a lifetime of about 10^{-10} s, while the $\Sigma^0(1192)$, a uds state decaying electromagnetically into $\Lambda\gamma$, has a lifetime of the order of 10^{-19} s, the basic transition being $u \to u\gamma$. The phase space for both decays is quite similar, and thus the difference in lifetime must be due to the difference of the couplings for the two interaction, being the amplitude (and thus the inverse of the lifetime) proportional to the square of the coupling. The comparison shows that the weak coupling is smaller by a factor of order of $\sim 10^{-4}$ with respect to the electromagnetic coupling. Although weak interactions take place between all quarks and leptons, the weak interaction is typically hidden by the much greater strong and electromagnetic interactions, unless these are forbidden by some conservation rule. Observable weak interactions involve either neutrinos or quarks with a flavor change—flavor change being forbidden in strong and electromagnetic interactions, since photons and gluons do not carry flavor.

The factor 10^{-4} is very interesting and suggests that the weak interactions might be weak because they are mediated by gauge fields, $W^\pm$ and Z, which are very massive and hence give rise to interactions of very short range. The strength of the interaction can be written as

$$f(q^2) = \frac{g_W^2}{q^2 + M^2} \,,$$

where M is the mass of the W or Z boson.

In the low-q^2 limit, the interaction is point-like, and the strength is given by the Fermi coupling $G_F \simeq 10^{-5}$ GeV^{-2}. The picture sketched above looks indeed consistent with the hypothesis that $g_W \sim e$ (we shall obtain a quantitative relation at the end of this Section). In fact

$$G_F \simeq \frac{e^2}{M_Z^2} \,.$$

Glashow[3] proposed in the 1960's—twenty years before the experimental discovery of the W and Z bosons—that the coupling of the W and Z to leptons and quarks is closely related to that of the photon; the weak and electromagnetic interactions are thus unified into an electroweak interaction. Mathematically, this unification is accomplished under a SU(2) $\otimes$ U(1) gauge group.

Weinberg, and Salam solved, in 1967, the problem given by the mass of the vector bosons: the photon is massless, while the W and Z bosons are highly massive. Indeed an appropriate spontaneous symmetry breaking of the electroweak Lagrangian explains the masses of the $W^{\pm}$ and of the Z keeping the photon massless and predicts the existence of a Higgs boson, which is called the standard model Higgs boson. The same Higgs boson can account for the masses of fermions. We shall see now how this unification is possible.

7.2.1 The Formalism of the Electroweak Theory

We used the symmetry group SU(2) to model weak interactions, while U(1) is the symmetry of QED. The natural space for a unified electroweak interaction appears thus to be SU(2) $\otimes$ U(1)—this is what the Glashow–Weinberg–Salam electroweak theory assumed at the end of the 1960s.

Let us call W^1, W^2, and W^0 the three gauge fields of SU(2). We call $W^a_{\mu\nu}$ ($a = 1, \ldots, 3$) the field tensors of SU(2) and $B_{\mu\nu}$ the field tensor of U(1). Notice that $B_{\mu\nu}$ is not equal to $F_{\mu\nu}$, in the same way as W^0 is not the Z field: since we use a tensor product of the two spaces, in general, the neutral field B can mix to the neutral field W^0, and the photon and Z states are a linear combination of the two.

The Lagrangian of the electroweak interaction needs to accommodate some experimental facts, which we have discussed in Chap. 6:

- Only the left-handed (right-handed) (anti)fermion chiralities participate in weak transitions—therefore, the interaction violates parity P and charge conjugation C; however, the combined CP transformation is still a good symmetry.
- The $W^{\pm}$ bosons couple to the left-handed fermionic doublets, where the electric charges of the two fermion partners differ in one unit. This leads to the following decay channels for the W^-:

[3] Sheldon Lee Glashow (New York City 1932) shared with Steven Weinberg (New York City 1933) and Abdus Salam (Jhang, Pakistan, 1926 - Oxford 1996) the Nobel Prize for Physics in 1979 "for their complementary efforts in formulating the electroweak theory. The unity of electromagnetism and the weak force can be explained with this theory." Glashow was the son of Jewish immigrants from Russia. He and Weinberg were members of the same classes at the Bronx High School of Science, New York City (1950), and Cornell University (1954); then Glashow became full professor in Princeton, and Weinberg in Harvard. Salam graduated in Cambridge, where he became full professor of mathematics in 1954, moving then to Trieste.

$$W^- \rightarrow e^-\bar{\nu}_e\,,\ \mu^-\bar{\nu}_\mu\,,\ \tau^-\bar{\nu}_\tau\,,\ d'\bar{u}\,,\ s'\bar{c}\,,\ b'\bar{t} \tag{7.19}$$

the latest being possible only as a virtual decay, since $m_t > m_W$.
The doublet partners of up, charm, and top are mixtures of the three charge $-\frac{1}{3}$ quarks:

$$\begin{pmatrix} d' \\ s' \\ b' \end{pmatrix} = V_{CKM} \begin{pmatrix} d \\ s \\ b \end{pmatrix} . \tag{7.20}$$

Thus, the weak eigenstates d', s', b' are different from the mass eigenstates d, s, b. They are related through the 3×3 unitary matrix V_{CKM}, which characterizes flavor-mixing phenomena.

- The neutral carriers of the electroweak interactions have fermionic couplings with the following properties:
  - All interacting vertices conserve flavor. Both the γ and the Z couple to a fermion and its own antifermion, i.e., $\gamma\, f\, \bar{f}$ and $Z\, f\, \bar{f}$.
  - The interactions depend on the fermion electric charge Q_f. Neutrinos do not have electromagnetic interactions ($Q_\nu = 0$), but they have a nonzero coupling to the Z boson.
  - Photons have the same interaction for both fermion chiralities.
- The strength of the interaction is universal, and lepton number is conserved.

We are ready now to draft the electroweak theory.

To describe weak interactions, the left-handed fermions should appear in doublets, and the right-handed fermions in singlets, and we would like to have massive gauge bosons $W^\pm$ and Z in addition to the photon. The simplest group with doublet representations having three generators is SU(2). The inclusion of the electromagnetic interactions implies an additional U(1) group. Hence, the symmetry group to consider is then

$$G \equiv \mathrm{SU}(2)_L \otimes \mathrm{U}(1)_Y\,, \tag{7.21}$$

where L refers to left-handed fields (this will represent the weak sector). We shall specify later the meaning of the subscript Y.

Let us first analyze the SU(2) part of the Lagrangian.

The $\mathrm{SU}(2)_L$ **part**. We have seen that the $W^\pm$ couple to the left chirality of fermionic doublets—what was called a $(V - A)$ coupling in the "old" scheme (Sect. 6.3.3). Let us start for simplicity our "modern" description from a leptonic doublet

$$\chi_L = \begin{pmatrix} \nu \\ e \end{pmatrix}_L .$$

Charged currents exist, coupling the members of the doublet:

$$j_\mu^+ = \bar{\nu}\gamma_\mu \left(\frac{1}{2}(1-\gamma_5)\right) e = \bar{\nu}_L \gamma_\mu e_L \tag{7.22}$$

$$j_\mu^- = \bar{e}\gamma_\mu \left(\frac{1}{2}(1-\gamma_5)\right) \nu = \bar{e}_L \gamma_\mu \nu_L \,. \tag{7.23}$$

These two currents are associated, for example, with weak decays of muons and neutrons. Notice that

$$\left(\frac{1}{2}(1-\gamma_5)\right)\left(\frac{1}{2}(1-\gamma_5)\right) = \left(\frac{1}{2}(1-\gamma_5)\right) ; \tag{7.24}$$

$$\left(\frac{1}{2}(1-\gamma_5)\right)\left(\frac{1}{2}(1+\gamma_5)\right) = 0 \,. \tag{7.25}$$

This should be evident by the physical meaning of these projectors; we leave for the Exercises a formal demonstration of these properties.

In analogy to the case of hadronic isospin, where the proton and neutron are considered as the two isospin eigenstates of the nucleon, we define a *weak isospin* doublet structure ($T = 1/2$)

$$\chi_L = \begin{pmatrix} \nu \\ e \end{pmatrix}_L \begin{matrix} T_3 = +1/2 \\ T_3 = -1/2 \end{matrix} , \tag{7.26}$$

with raising and lowering operators between the two components of the doublet

$$\tau_\pm = \frac{1}{2}(\tau_1 \pm i\tau_2) \tag{7.27}$$

where the τ_i are the Pauli matrices.

The same formalism applies to a generic quark doublet, for example

$$\chi_L = \begin{pmatrix} u \\ d' \end{pmatrix}_L \begin{matrix} T_3 = +1/2 \\ T_3 = -1/2 \end{matrix} . \tag{7.28}$$

With this formalism, we can write the charged currents as

$$j_\mu^+ = \bar{\chi}_L \gamma_\mu \tau_+ \chi_L \tag{7.29}$$

$$j_\mu^- = \bar{\chi}_L \gamma_\mu \tau_- \chi_L \,. \tag{7.30}$$

When imposing the SU(2) symmetry, one has two vector fields W^1 and W^2 corresponding to the Pauli matrices τ_1 and τ_2. Notice that they do not correspond necessarily to "good" particles, since, for example, they are not necessarily eigenstates of the electric charge operator. However, we have seen that they can be combined to physical states corresponding to the charged currents $W^\pm$ (Eq. 7.27):

$$W^{\pm} = \sqrt{\frac{1}{2}}(W^1 \pm i W^2)\,. \tag{7.31}$$

A third vector field W^0 associated to the third generator τ_3 corresponds to a neutral transition (analogous to the π^0 in the case of the isospin studied for strong interactions):

$$j^3_\mu = \bar{\chi}_L \gamma_\mu \left(\frac{1}{2}\tau_3\right) \chi_L\,. \tag{7.32}$$

We have finally a triplet of currents

$$j^i_\mu = \bar{\chi}_L \gamma_\mu \left(\frac{1}{2}\tau_i\right) \chi_L \tag{7.33}$$

with algebra

$$[\tau_i, \tau_j] = i\epsilon_{ijk}\tau_k\,; \tag{7.34}$$

from this, we can construct the Lagrangian according to the recipes in Sect. 6.4.1. Before doing so, let us examine the U(1) part of the Lagrangian.

The $\mathrm{U}(1)_Y$ **part**. The electromagnetic current

$$j^{em}_\mu = \bar{e}\gamma_\mu e = \bar{e}_L \gamma_\mu e_L + \bar{e}_R \gamma_\mu e_R$$

is invariant under $\mathrm{U}(1)_Q$, the gauge group of QED associated to the electromagnetic charge. It is, however, not invariant under $\mathrm{SU}(2)_L$: it contains e_L instead of χ_L.

The neutral isospin

$$j^3_\mu = \bar{\chi}_L \gamma_\mu \left(\frac{1}{2}\tau_3\right) \chi_L = \bar{\nu}_L \left(\frac{1}{2}\gamma_\mu\right) \nu_L - \bar{e}_L \left(\frac{1}{2}\gamma_\mu\right) e_L \tag{7.35}$$

couples only left-handed particles, while we know that neutral current involves both chiralities.

To have a consistent picture, we must construct a $\mathrm{SU}(2)_L$-invariant U(1) current. We define a *hypercharge*

$$Y = 2(Q - T_3)\,. \tag{7.36}$$

We can thus write

$$j^Y_\mu = 2j^{em}_\mu - 2j^3_\mu = -2\bar{e}_R \gamma_\mu e_R - \bar{\chi}_L \gamma_\mu \chi_L\,. \tag{7.37}$$

The last expression is invariant with respect to $\mathrm{SU}(2)_L$ (e_R is a weak hypercharge singlet).

Construction of the Electroweak Lagrangian. The part of the Lagrangian related to the interaction between gauge fields and fermion fields can now be written as

$$\mathcal{L}_{int} = -ig j_\mu^a W^{a\mu} - i\frac{g'}{2} j_\mu^Y B^\mu \,, \tag{7.38}$$

while the part related to the gauge field is

$$\mathcal{L}_g = -\frac{1}{4} W_a^{\mu\nu} W^a_{\mu\nu} - \frac{1}{4} B^{\mu\nu} B_{\mu\nu} \,, \tag{7.39}$$

where $W^{a\mu\nu} (a = 1, 2, 3)$ and $B^{\mu\nu}$ are the field strength tensors for the weak isospin and weak hypercharge fields. In the above, we have called g the strength of the SU(2) coupling, and g' the strength of the hypercharge coupling. The field tensors above can be explicitly written as

$$W^a_{\mu\nu} = \partial_\mu W^a_\nu - \partial_\nu W^a_\mu - g\, f^{bca} W^b_\mu W^c_\nu \tag{7.40}$$

$$B_{\mu\nu} = \partial_\mu B_\nu - \partial_\nu B_\mu \,. \tag{7.41}$$

Finally, including the kinetic part, the Lagrangian can be written as

$$\mathcal{L}_0 = \sum_{\text{families}} \overline{\chi}_f (i\gamma^\mu D_\mu) \chi_f - \frac{1}{4} W^a_{\mu\nu} W^{a\mu\nu} - \frac{1}{4} B_{\mu\nu} B^{\mu\nu} \,, \tag{7.42}$$

with

$$D_\mu = \partial_\mu + igW^a_\mu \frac{\tau^a}{2} + ig' Y B_\mu \,. \tag{7.43}$$

At this point, the four gauge bosons W^a and B are massless. But we know that the Higgs mechanism can solve this problem.

In addition, we did not introduce fermion masses, yet. When discussing electromagnetism and QCD as gauge theories, we put fermion masses "by hand" in the Lagrangian. This is not possible here, since an explicit mass term would break the SU(2) symmetry. A mass term $-m_f \overline{\chi}_f \chi_f$ for each fermion f in the Lagrangian would give, for the electron for instance,

$$-m_e \bar{e} e = -m_e \bar{e} \left(\frac{1}{2}(1 - \gamma_5) + \frac{1}{2}(1 + \gamma_5) \right) e = -m_e (\bar{e}_R e_L + \bar{e}_L e_R) \tag{7.44}$$

which is noninvariant under the isospin symmetry transformations, since e_L is a member of an $\mathrm{SU(2)_L}$ doublet while e_R is a singlet.

We shall see that fermion masses can come "for free" from the Higgs mechanism.

7.2.2 The Higgs Mechanism in the Electroweak Theory and the Mass of the Electroweak Bosons

In Sect. 7.1.4, the Higgs mechanism was used to generate a mass for the gauge boson corresponding to a U(1) local gauge symmetry. In this case, three Goldstone bosons will be required (we need them to give mass to W^+, W^-, and Z). In addition, after symmetry breaking, there will be (at least) one massive scalar particle corresponding to the field excitations in the direction picked out by the choice of the physical vacuum.

The simplest Higgs field, which has the necessary four degrees of freedom, consists of two complex scalar fields, placed in a weak isospin doublet. One of the scalar fields will be chosen to be charged with charge +1 and the other to be neutral. The hypercharge of the doublet components will thus be $Y = 2(Q - T_3) = 1$. The Higgs doublet is then written as

$$\phi = \begin{pmatrix} \phi^+ \\ \phi^0 \end{pmatrix} = \frac{1}{\sqrt{2}} \begin{pmatrix} \phi_1 + i\phi_2 \\ \phi_3 + i\phi_4 \end{pmatrix} . \tag{7.45}$$

We choose as a vacuum the point $\phi_1 = \phi_2 = \phi_4 = 0$ and $\phi_3 = v$, and we expand

$$\phi(x) = \frac{1}{\sqrt{2}} \begin{pmatrix} 0 \\ v + h(x) \end{pmatrix} .$$

To the SM Lagrangian discussed in the previous subsection (Eq. 7.42), we need to add the Higgs potential $V(\phi)$. We obtain, in a compact form, for the free Higgs Lagrangian:

$$\begin{aligned} \mathcal{L}_{\text{Higgs}} &= (D^\mu \phi)^\dagger (D_\mu \phi) - V(\phi^\dagger \phi) \\ &= (D^\mu \phi)^\dagger (D_\mu \phi) - \mu^2 \phi^\dagger \phi - \lambda (\phi^\dagger \phi)^2 . \end{aligned} \tag{7.46}$$

with the covariant derivative D_μ given by Eq. 7.43.

After SSB, this Lagrangian can be approximated around the minimum as

$$\begin{aligned} \mathcal{L}_{\text{free}} &= \text{constant} + \text{kinetic terms} + \\ &+ \frac{1}{2} (-2\mu^2)\, h^2 && (7.47) \\ &+ \frac{1}{2} \left(\frac{1}{4} g^2 v^2 \right) W^1_\mu \, W^{1\mu} + \frac{1}{2} \left(\frac{1}{4} g^2 v^2 \right) W^2_\mu \, W^{2\mu} && (7.48) \\ &+ \frac{1}{8} v^2 \left(W^{3\mu} \; B^\mu \right) \begin{pmatrix} g^2 & -gg'Y \\ -gg'Y & g'^2 \end{pmatrix} \begin{pmatrix} W^3_\mu \\ B_\mu \end{pmatrix} && (7.49) \\ &+ \mathcal{O}(3) , \end{aligned}$$

where as in the case of Sect. 7.1.4, we have introduced the new field around the point of minimum (we call it h instead of σ).

- As usual in the SSB, the h field acquires mass; we shall call the corresponding particle H. This is the famous standard model Higgs boson, and its mass is

$$m_H = \sqrt{-2\mu^2} = \sqrt{2\lambda}v\,. \tag{7.50}$$

- We now analyze the term (7.48). We have two massive charged bosons W^1 and W^2 with the same mass $gv/2$. We have seen, however, that physical states of integer charge ± 1 can be constructed by a linear combination of them (Eq. 7.31):

$$W^{\pm} = \sqrt{\frac{1}{2}}(W^1 \pm i\,W^2)\,.$$

The mass is as well

$$M_{W^{\pm}} = \frac{1}{2}\,gv\,, \tag{7.51}$$

and these states correspond naturally to the charged current vectors.

- Finally, let us analyze the term (7.49).
Here, the fields W^3 and B couple through a nondiagonal matrix; they thus are not mass eigenstates. The physical fields can be obtained by an appropriate rotation which diagonalizes the mass matrix

$$M = \begin{pmatrix} g^2 & -gg'Y \\ -gg'Y & g'^2 \end{pmatrix}\,.$$

For $Y = \pm 1$ (we recall our choice $Y = 1$), the determinant of the matrix is 0, and when we shall diagonalize, one of the two eigenstates will be massless. If we introduce the fields A_μ and Z_μ defined as

$$A_\mu \;= \sin\theta_W\, W^0_\mu + \cos\theta_W\, B_\mu \tag{7.52}$$

$$Z_\mu = \cos\theta_W\, W^0_\mu - \sin\theta_W\, B_\mu\,, \tag{7.53}$$

where the angle θ_W, the weak mixing angle first introduced by Glashow but often called the Weinberg angle (also known as weak angle), parametrizes the electroweak mixing:

$$\tan\theta_W = \frac{g'}{g}\,, \tag{7.54}$$

the term (7.49) becomes

$$\frac{1}{8}\,v^2\,(A^\mu\;Z^\mu)\begin{pmatrix} 0 & 0 \\ 0 & g^2+g'^2 \end{pmatrix}\begin{pmatrix} A_\mu \\ Z_\mu \end{pmatrix}\,. \tag{7.55}$$

A_μ is then massless (we can identify it with the photon). Note that

$$M_Z = \frac{1}{2}\, v\sqrt{g^2 + g'^2}\,, \tag{7.56}$$

and thus

$$M_W = M_Z\, \cos\theta_W\,. \tag{7.57}$$

From the above expression, using the measured masses of the W and Z bosons, we can get an estimate of the Weinberg angle:

$$\sin^2\theta_W \simeq 1 - \left(\frac{M_W}{M_Z}\right)^2 \simeq 1 - \left(\frac{80.385\,\text{GeV}}{91.188\,\text{GeV}}\right)^2 \simeq 0.22\,. \tag{7.58}$$

Note the use of $\simeq$ symbols: this result has been obtained only at tree level of the electroweak theory, while in the determination of the actual masses of the W and Z, boson higher-order terms enter, related, for example, to QCD loops. Higher-order processes ("radiative corrections") should be taken into account to obtain a fully consistent picture, see later; the current "best fit" value of the Weinberg angle provides

$$\sin^2\theta_W = 0.2318 \pm 0.0006\,. \tag{7.59}$$

Electric charge is obviously conserved, since it can be associated to a generator which is the linear combination of the isospin generator and of the generator of hypercharge. For eigenvectors of SU(2) $\otimes$ U(1), one has

$$Q = Y + \frac{T_3}{2}\,. \tag{7.60}$$

Thus the covariant derivative can be written as

$$\begin{aligned} D_\mu &= \left(\partial_\mu + i g W_\mu^a \frac{\tau^a}{2} + i g' \frac{1}{2} B_\mu\right) = \\ &= \partial_\mu + i\frac{g}{\sqrt{2}}\, W_\mu^+ \tau^+ + \frac{g}{\sqrt{2}}\, W^- \tau^- + i g \sin\theta_W\, Q A_\mu + i\frac{g}{\cos\theta_W}\, \left(\frac{\tau_3}{2} - \sin^2\theta_W\, Q\right) Z_\mu \end{aligned} \tag{7.61}$$

and thus

$$g \sin\theta_W = e\,. \tag{7.62}$$

The above relation holds also at tree level only: we shall see in Sect. 7.4 that radiative corrections can influence at a measurable level the actual values of the observables in the standard model.

7.2.3 The Fermion Masses

Up to now the fermion fields in the theory are massless, and we have seen (Eq. 7.44) that we cannot insert them by hand in the Lagrangian as we did in the case of QED and QCD. A simple way to explain the fermion masses consistent with the electroweak interaction is to ascribe such a mass to the Higgs mechanism, again: masses appear after the SSB.

The problem can be solved by imposing in the Lagrangian coupling of the Higgs doublet to the fermions by means of gauge invariant terms like (for the electron)

$$\mathcal{L}_{eeh} = -\frac{\lambda_e}{\sqrt{2}}\left[(\bar{\nu}_e, \bar{e})_L \begin{pmatrix} 0 \\ v+h \end{pmatrix} e_R + \bar{e}_R(0, v+h)\begin{pmatrix} \nu_e \\ e \end{pmatrix}_L\right]. \tag{7.63}$$

This generates fermion mass terms and Higgs–fermion interaction terms:

$$\mathcal{L}_{eeh} = -\frac{\lambda_e v}{\sqrt{2}}\bar{e}e \; - \frac{\lambda_e}{\sqrt{2}}\bar{e}e\,h\,. \tag{7.64}$$

Since the symmetry breaking term λ_f for each fermion field is unknown, the masses of fermions in the theory are free parameters and must be determined by experiment. Setting $\lambda_f = \sqrt{2}m_f/v$, the part of the Lagrangian describing the fermion masses and the fermion–Higgs interaction for each fermion is

$$\mathcal{L}_{ffh} = -m_f\,\bar{f}f \; - \frac{m_f}{v}\,\bar{f}f\,h\,. \tag{7.65}$$

Notice that the coupling to the Higgs is proportional to the mass of the fermion: this is a strong prediction, to be verified by experiment.

We stress the fact that we need just one Higgs field to explain all massive particles of the standard model: the weak vector bosons $W^{\pm}$, Z, fermions, and the Higgs boson itself. The electromagnetic symmetry and the SU(3) color symmetry both remain unbroken—the former being an accidental symmetry of $\mathrm{SU}(2)_L \otimes \mathrm{U}(1)_Y$. This does not exclude, however, that additional Higgs fields exist—it is just a matter of economy of the theory, or, if you prefer, it is just a consequence of the Occam's razor, to the best of our present knowledge.

7.2.4 Interactions Between Fermions and Gauge Bosons

Using Eq. 7.61, we can write the interaction terms between the gauge bosons and the fermions (we use a lepton doublet as an example, but the result is general) as

$$\begin{aligned}\mathcal{L}_{\text{int}} = &-\frac{g}{2\sqrt{2}}\,\overline{\nu}_e\gamma^\mu(1-\gamma_5)e\,W^+_\mu - \frac{g}{2\sqrt{2}}\,\overline{e}\gamma^\mu(1-\gamma_5)\nu_e\,W^-_\mu \\ &- \frac{g}{4\cos\theta_W}\left[\overline{\nu}_e\,\gamma^\mu(1-\gamma_5)\nu_e - \overline{e}\gamma^\mu(1-4\sin^2\theta_W\ -\gamma_5)e\right]Z_\mu \\ &- (-e)\,\overline{e}\gamma^\mu e\,A_\mu\,. \end{aligned} \tag{7.66}$$

The term proportional A_μ is the QED interaction.

Usually, the Z interaction in Eq. 7.66 is written (for a generic fermion f) as

$$\begin{aligned}\mathcal{L}^Z_{\text{int}} &= -\frac{g}{\cos\theta_W}\left[\overline{\nu}_e\gamma^\mu(g^\nu_V - g^\nu_A\gamma_5)\nu_e + \overline{e}\gamma^\mu(g^e_V - g^e_A\gamma_5)e\right]Z^\mu \\ &\quad + \text{ other fermions} \\ &= -\frac{g}{\cos\theta_W}\sum_f \overline{\chi}_f\gamma^\mu(g^f_V - g^f_A\gamma_5)\chi_f Z_\mu \end{aligned} \tag{7.67}$$

from which we define the couplings

$$g^f_V = \frac{1}{2}T^f_3 - Q^f\sin^2\theta_W\,; \qquad g^f_A = \frac{1}{2}T^f_3\,. \tag{7.68}$$

The Z interaction can also be written considering the left and right helicity states of the fermions. Indeed, for a generic fermion f,

$$\begin{aligned}&\overline{\psi}_f\gamma^\mu(g^f_V - g^f_A\gamma_5)\psi_f = \\ &= \overline{\psi}_f\gamma^\mu\left[\frac{1}{2}(g^f_V + g^f_A)(1-\gamma_5) + \frac{1}{2}(g^f_V - g^f_A)(1+\gamma_5)\right]\psi_f = \\ &= \overline{\psi}_{fL}\gamma^\mu g_L\psi_{fL} + \overline{\psi}_{fR}\gamma^\mu g_R\psi_{fR} \end{aligned} \tag{7.69}$$

where the left and right couplings g_L and g_R are thus given by

$$g_L = \frac{1}{2}(g_V + g_A) \tag{7.70}$$

$$g_R = \frac{1}{2}(g_V - g_A)\,. \tag{7.71}$$

In the case of neutrinos, $Q = 0$, $g_V = g_A$, and thus $g_R = 0$. The right neutrino has then no interaction with the Z and as, by construction, it has also no interactions with the γ, $W^\pm$, and gluons. The right neutrino is therefore, if it exists, *sterile*.

On the contrary, for electrical charged fermions, $g_V \neq g_A$ and thus the Z boson couples both with left and right helicity states although with different strengths ($g_L \neq g_R \neq 0$).

Parity is also violated in the Z interactions.

These results are only valid in the one-family approximation. When extending to three families, there is a complication: in particular, the current eigenstates for

quarks q' are not identical to the mass eigenstates q. If we start by u-type quarks being mass eigenstates, in the down-type quark sector, the two sets are connected by a unitary transformation

$$(d', s', b') = V_{\mathrm{CKM}}(d, s, b)\,. \tag{7.72}$$

Let us compute as an example the differential cross section for processes involving electroweak currents. We should not discuss the determination of the absolute value, but just the dependence on the flavor and on the angle.

Let us examine the fermion antifermion, $f\bar{f}$, production in e^+e^- annihilations.

At a center-of-mass energy smaller than the Z mass, the photon coupling will dominate the process. The branching fractions will be dominated by photon exchange and thus proportional to Q_f^2 (being zero in particular for neutrinos).

Close to the Z mass, the process will be dominated by decays $Z \to f\bar{f}$ and the amplitude will be proportional to $(g_V^f + g_A^f)$ and $(g_V^f - g_A^f)$, respectively, for left and right fermions. The width into $f\bar{f}$ will be then proportional to

$$\left[(g_V^f + g_A^f)^2 + (g_V^f - g_A^f)^2\right] = {g_V^f}^2 + {g_A^f}^2. \tag{7.73}$$

Hence:

$$\Gamma_{f\bar{f}} \simeq \frac{M_Z}{12\pi}\left(\frac{g}{\cos\theta_W}\right)^2\left[{g_V^f}^2 + {g_A^f}^2\right]. \tag{7.74}$$

Expressing the result in terms of the Fermi constant

$$\frac{G_F}{\sqrt{2}} = \frac{g^2}{8M_W^2} = \left(\frac{g}{\cos\theta_W}\right)^2\frac{1}{8M_Z^2} \tag{7.75}$$

one has

$$\Gamma = \frac{2G_F M_Z^3}{3\sqrt{2}\pi}\left[{g_V^f}^2 + {g_A^f}^2\right]. \tag{7.76}$$

For example, for $\mu^+\mu^-$ pairs,

$$\Gamma(Z \to \mu^+\mu^-) \simeq 83.4\,\mathrm{MeV}\,. \tag{7.77}$$

As a consequence of parity violation in electroweak interactions, a forward–backward asymmetry will characterize the Z decays into $f\bar{f}$. The forward–backward asymmetry for the decay of a Z boson into a fermion pair is[4] in the core of unpolarized electron/positron beams,

[4]For a deduction, see, for instance, Chap. 16.2 of Reference [F7.2] in the "Further readings".

$$A_{FB}^{f} \equiv \left[\int_0^{+1} \frac{\mathrm{d}\sigma}{\mathrm{d}\cos\theta} - \int_{-1}^{0} \frac{\mathrm{d}\sigma}{\mathrm{d}\cos\theta}\right] / \sigma_{\mathrm{tot}} \overset{\sqrt{s}=M_Z}{\simeq} \frac{3}{4} A_e A_f \tag{7.78}$$

where the combinations A_f are given, in terms of the vector and axial vector couplings of the fermion f to the Z boson, by

$$A_f = \frac{2 g_V^f g_A^f}{g_V^{f\,2} + g_A^{f\,2}}\,, \tag{7.79}$$

and A_e is the corresponding combination for the specific case of the electron.

The tree-level expressions discussed above give results which are correct at the percent level, in the case of b quark final states, additional mass effects $\mathcal{O}(4m_b^2/M_Z^2)$, also $\sim$0.01, have to be taken into account. For the production of e^+e^- final states, the t-channel gauge boson exchange contributions have to be included (this process allows to determine the absolute luminosity at e^+e^- colliders, making it particularly important), and it is dominant at low angles, the cross section being proportional to $\sin^3\theta$. However, one needs to include the one-loop radiative corrections so that the Z properties can be described accurately, and possibly some important higher-order effects, which will be shortly discussed later.

7.2.5 *Self-interactions of Gauge Bosons*

Self-couplings among the gauge bosons are present in the SM as a consequence of the nonabelian nature of the $\mathrm{SU(2)_L} \otimes \mathrm{U(1)_Y}$ symmetry. These couplings are dictated by the structure of the symmetry group as discussed before, and, for instance, the triple self-couplings among the W and the $V = \gamma, Z$ bosons are given by

$$\mathcal{L}_{WWV} = i g_{WWV} \left[W_{\mu\nu}^{\dagger} W^{\mu} B^{\nu} - W_{\mu}^{\dagger} B_{\nu} W^{\mu\nu} + W_{\mu}^{\dagger} W_{\nu} B^{\mu\nu}\right] \tag{7.80}$$

with $g_{WW\gamma} = e$ and $g_{WWZ} = e/\tan\theta_W$.

7.2.6 *Feynman Diagram Rules for the Electroweak Interaction*

We have already shown how to compute the invariant amplitude $\mathcal{M}$ for a scalars fields in Sect. 6.2.7. We give here only the Feynman rules for the propagators (Fig. 7.4) and vertices (Fig. 7.5) of the standard model that we can use in our calculations—or our estimates, since the calculation of the complete amplitude including spin effects can be very lengthy and tedious. We follow here Ref. [F7.5] in the "Further readings"; a complete treatment of the calculation of amplitudes from the Feynman diagrams

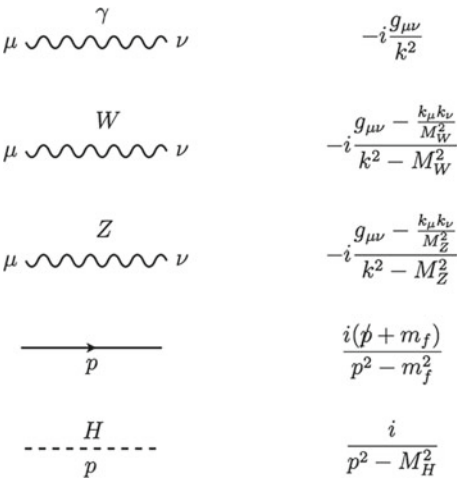

Fig. 7.4 Terms associated to propagators in the electroweak model. From [F7.5]

can be found in Ref. [F7.1]. Note that we do not provide QCD terms, since the few perturbative calculations practically feasible in QCD involve a very large number of graphs.

7.3 The Lagrangian of the Standard Model

The Lagrangian of the standard model is the sum of the electroweak Lagrangian (including the Higgs terms, which are responsible for the masses of the $W^{\pm}$ bosons and of the Z, and of the leptons) plus the QCD Lagrangian without the fermion mass terms.

7.3.1 The Higgs Particle in the Standard Model

The SM Higgs boson is thus the Higgs boson of the electroweak Lagrangian.

In accordance with relation (7.65), the interaction of the Higgs boson with a fermion is proportional to the mass of this fermion itself: $g_{\mathrm{Hff}} = \dfrac{m_f}{v}$.

One finds that the Higgs boson couplings to the electroweak gauge bosons are instead proportional to the squares of their masses:

$$g_{HWW} = 2\frac{M_W^2}{v}, \quad g_{HHWW} = \frac{M_W^2}{v^2}, \quad \text{and} \quad g_{HZZ} = \frac{M_Z^2}{v}, \quad g_{HHZZ} = \frac{M_Z^2}{2v^2}\,. \tag{7.81}$$

Charged Current

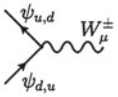

$$-i\frac{g}{\sqrt{2}}\gamma_\mu\frac{1-\gamma_5}{2}$$

Neutral Current

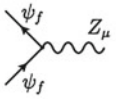

$$-i\frac{g}{\cos\theta_W}\gamma_\mu\left(g_V^f-g_A^f\gamma_5\right)$$

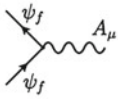

$$-ieQ_f\gamma_\mu$$

where

$$g_V^f=\frac{1}{2}T_f^3-Q_f\sin^2\theta_W,\quad g_A^f=\frac{1}{2}T_f^3\,.$$

Higgs Interactions

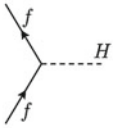

$$-i\frac{g}{2}\frac{m_f}{M_W}=-i\frac{m_f}{v}$$

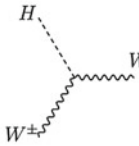

$$ig\,M_W=2i\frac{M_W^2}{v}$$

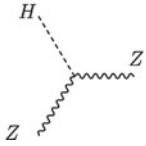

$$i\frac{g}{2\cos\theta_W}M_Z=i\frac{M_Z^2}{v}$$

Fig. 7.5 Terms associated to vertices in the electroweak model. Adapted from [F7.5]

Among the consequences, the prediction of the branching fractions for the decay of the Higgs boson is discussed later.

7.3.2 Standard Model Parameters

The standard model describes in detail particle physics at least at energies below or at the order of the electroweak scale (gravity is not considered here). Its power has been intensively and extensively demonstrated in the past thirty years by an impressive

number of experiments (see later in this Chapter). However, it has a relatively large set of "magic numbers" not defined by the theory, which thus have to be obtained from measurements. The numerical values of these parameters were found to differ by more than ten orders of magnitude (e.g., $m_\nu < 0.1\,\text{eV}$, $m_t \sim 0.2\,\text{TeV}$).

These free parameters may be listed in the hypothesis that neutrinos are standard massive particles (the hypothesis that they are "Majorana" particles, i.e., fermions coincident with their antiparticles, will be discussed in Chap. 9), as follows:

- In the gauge sector:
  - three gauge constants (respectively, $\text{SU}(2)_L$, $\text{U}(1)_Y$, $\text{SU}(3)$):

$$g,\ g',\ g_s\,.$$

- In the Higgs sector:
  - the two parameters of the standard Higgs potential:

$$\mu,\ \lambda\,.$$

- In the fermionic sector:
  - the twelve fermion masses (or alternatively the corresponding Higgs–fermion Yukawa couplings):

$$m_{\nu 1}, m_{\nu 2}, m_{\nu 3}, m_e, m_\mu, m_\tau, m_u, m_d, m_c, m_s, m_t, m_b\ ;$$

  - the four quark CKM mixing parameters (in the Wolfenstein parametrization; see Sect. 6.3.7):

$$\lambda,\ A,\ \rho,\ \eta\,;$$

  - the four neutrino PMNS mixing parameters (see Sect. 9.1.1), which can be three real angles and one phase:

$$\theta_{12},\ \theta_{13},\ \theta_{23},\ \delta\,.$$

- In the strong CP sector:
  - A "CP violating phase" θ_{CP}. The U(1) symmetry cannot host CP violation (one can easily see it in this case since there is no room for the addition of nontrivial complex phases; a general demonstration holds for Abelian groups). We know instead that the electroweak sector contains a CP-violating phase. In principle, the QCD Lagrangian could also have a CP-violating term $i\,\theta_{CP}\epsilon_{\mu\nu\rho\sigma}F_a^{\mu\nu}F_a^{\rho\sigma}$; experiments tell, however, that the effective CP violation in strong interactions, if existing, is extremely small ($\theta_{CP,\,\text{eff}} < 10^{-10}$). It is common then to assume

$$\theta_{CP} = 0\,. \tag{7.82}$$

It is difficult to imagine why the value of θ_{CP} should be accidentally so small—or zero: this is called the "strong CP problem." A viable solution would be to introduce an extra symmetry in the Lagrangian, and this was the solution proposed by Peccei and Quinn in the 1970s. An extra symmetry, however, involves a new gauge boson, which was called the axion; the axion should possibly be observed to confirm the theory.

However, the choice of the 26 "fundamental" parameters is somehow arbitrary because there are several quantities that are related to each other. In the Higgs sector, the vacuum expectation value v is often used; in the gauge sector, α, G_F, and α_s are the most common "experimental" choices to describe the couplings of the electromagnetic, weak interaction, and strong interaction; finally, $\sin^2\theta_W$ is for sure one of the most central quantities measured in the different decays or interaction channels. Indeed

$$v = \sqrt{-\frac{\mu^2}{\lambda}} \; ; \; \tan(\theta_W) = \frac{g'}{g} \; ; \; \alpha = \frac{e^2}{4\pi} = \frac{(g \sin\theta_W)^2}{4\pi} \; ; \; G_F = \frac{1}{\sqrt{2}\, v^2} \; ; \; \alpha_s = \frac{{g_s}^2}{4\pi} .$$

The bare masses of the electroweak gauge bosons, as well as their couplings, are derived directly from the standard model Lagrangian after the Higgs spontaneous symmetry breaking mechanism (see the previous sections):

- $m_\gamma = 0$, by construction
- $m_Z = \frac{1}{2}\sqrt{g^2 + g'^2}\, v$
- $m_W = \frac{1}{2} g v$

and $\sin^2\theta_W$ can also be expressed as

$$\sin^2\theta_W = 1 - \frac{{m_W}^2}{{m_Z}^2} = \frac{\pi\alpha}{\sqrt{2} G_F {m_W}^2} = \frac{\pi\alpha}{\sqrt{2} G_F {m_Z}^2 \cos^2\theta_W} . \tag{7.83}$$

The couplings of the electroweak gauge bosons to fermions were discussed in Sect. 7.2.4 and are proportional to

- $e = g \sin\theta_W$ for the photon γ;
- g, for the $W^\pm$ which only couples to left-handed fermions;
- $g/\cos\theta_W \; (g_V + g_A)$ and $g/\cos\theta_W \; (g_V - g_A)$ for the Z, respectively, for couplings to left and right fermions. $g_V = I_3 - 2\, Q_f \sin^2\theta_W$ and $g_A = I_3$ being Q_f and I_3, respectively, the electric charge and the third component of the weak isospin of the concerned fermion.

Finally, the mass of the Higgs boson is given, as seen Sect. 7.2.2, by

$$m_H = \sqrt{2\lambda} v . \tag{7.84}$$

7.3.3 *Accidental Symmetries*

The standard model exhibits additional global symmetries, collectively denoted accidental symmetries, which are continuous U(1) global symmetries which leave the Lagrangian invariant. By Noether's theorem, each symmetry has an associated conserved quantity; in particular, the conservation of baryon number (where each quark is assigned a baryon number of 1/3, while each antiquark is assigned a baryon number of $-1/3$), electron number (each electron and its associated neutrino is assigned an electron number of $+1$, while the antielectron and the associated antineutrino carry a -1 electron number), muon number, and tau number are accidental symmetries. Note that somehow these symmetries, although mathematically "accidental," exist by construction, since, when we designed the Lagrangian, we did not foresee gauge particles changing the lepton number or the baryon number as defined before.

In addition to the accidental symmetry, but nevertheless exact symmetries, described above, the standard model exhibits several approximate symmetries. Two of them are particularly important:

- The SU(3) quark flavor symmetry, which reminds us the symmetries in the "old" hadronic models. This obviously includes the SU(2) quark flavor symmetry—the strong isospin symmetry, which is less badly broken (only the two light quarks being involved).
- The SU(2) custodial symmetry, which keeps

$$r = \frac{{m_W}^2}{{m_Z}^2 \cos^2 \theta_W} \simeq 1$$

limiting the size of the contributions from loops involving the Higgs particle (see the next Section). This symmetry is exact before the SSB.

7.4 Observables in the Standard Model

As it was discussed in the case of QED (see Sect. 6.2.9), measurable quantities are not directly bare quantities present in the Lagrangian, but correspond to effective quantities which "absorb" the infinities arising at each high-order diagrams due to the presence of loops for which integration over all possible momentum should be performed. These effective renormalized quantities depend on the energy scale of the measurement. This was the case for α and α_s as discussed in Sects. 6.2.10 and 6.4.4. The running of the electromagnetic coupling α

$$\alpha\left({m^2}_e\right) \sim \frac{1}{137};\ \alpha\left({m^2}_Z\right) \sim \frac{1}{129}$$

implies, for instance, a sizeable change on the values of m_Z and m_W from those that could be computed using the relations listed above ignoring this running and taking for G_F and $\sin^2\theta_W$ the values measured at low energy (muon decay for G_F and deep inelastic neutrino scattering for s_W).

In addition, QCD corrections to processes involving quarks can be important. For example, at the first perturbative order α_s (essentially keeping into account the emission of one gluon)

$$\frac{\Gamma(Z \to q\bar{q})}{\Gamma(Z \to q\bar{q})_{\text{leading}}} \simeq 1 + \frac{\alpha_s}{\pi}\,; \tag{7.85}$$

radiation of quarks and gluons increases the decay amplitude linearly in α_s. In fact these QCD corrections are known to $\mathcal{O}(\alpha_s^3)$ for $\Gamma_{q\bar{q}}$ (see later), and the measurement of the hadronic Z width provides the most precise estimate of α_s—see later a better approximation of Eq. 7.85.

High-order diagrams have thus to be carefully computed in order that the high-precision measurements that have been obtained in the last decades (see the next section) can be related to each other and, in that way, determine the level of consistency (or violation) of the standard model. These corrections are introduced often as a modification of previous lowest order formulas as, for example,

$$\sin^2\theta_W \cos^2\theta_W = \frac{\pi\alpha}{\sqrt{2}G_F m_Z{}^2\,(1-\Delta r)} \tag{7.86}$$

and detailed calculations provide

$$\Delta r \;\sim -\frac{3\alpha}{16\pi \sin^4\theta_W}\,\frac{m_t{}^2}{m_Z{}^2} + \frac{11\alpha}{24\pi \sin^2\theta_W}\ln\left(\frac{m_H}{m_Z}\right) + \cdots . \tag{7.87}$$

The determination of Δr or of any electroweak correction is far beyond the scope of the present book. We just stress that Δr, and most of the radiative corrections, are in the largest part an effect of loops involving top quarks and Higgs particles. These enter in the calculations as $m_t{}^2$ and $\ln(m_H)$, respectively, and the total effect is at a some percent level. The quadratic dependence on m_t may appear as a surprise since in QED the contributions of loops involving heavy fermions are suppressed by inverse powers of the fermion mass. $SU(2)_L$ is however a chiral broken symmetry (the masses of the fermions are not degenerated) and, for instance, the self-energy corrections to the W propagator involving $t\,\bar{b}$ (or $\bar{t}\,b$) loops (Fig. 7.6) are proportional to $\left(m_t{}^2 - m_b{}^2\right)$. Both the quadratic dependence on m_t as well as the logarithmic dependence on m_H are a consequence of the way how the Higgs sector and the symmetry breaking mechanism are built in the standard model, leaving a remnant approximate symmetry (the "custodial" symmetry we examined in the previous section).

In addition, Δr can be sensitive to "new physics": the presence of additional virtual loops involving yet undiscovered particles affects the radiative corrections.

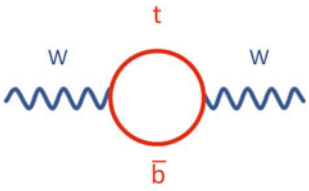

Fig. 7.6 $t\,\bar{b}$ loop contributing to self-energy corrections to the W propagator

In a similar way, an electroweak form factor ρ_Z^f can be introduced to account for higher-order corrections to the Z couplings:

$$g_V = \sqrt{\rho_Z^f}\,\left(I_3 - 2\,Q_f \sin^2\theta_W\right) \tag{7.88}$$

$$g_A = \sqrt{\rho_Z^f}\,I_3\,. \tag{7.89}$$

The departure of ρ_Z^f from the unity ($\Delta\rho_Z^f$) is again a function of ${m_t}^2$ and $\ln(m_H)$.

Another way to incorporate radiative corrections in the calculations, frequently used in the literature, is to absorb them in the Weinberg angle, which then becomes an "effective" quantity. The form of the calculations then stays the same as that at leading order, but with an "effective" angle instead of the "bare" angle.

This approach is the simplest—and probably the most common in the literature—but one has to take into account that, at higher orders, the "effective" value of the angle will be different for different processes.

Global fits to electroweak precision data (see, for instance, the Gfitter project at CERN), taking properly into account correlations between standard model observables, have so far impressively shown the consistency of the standard model and its predictive power.

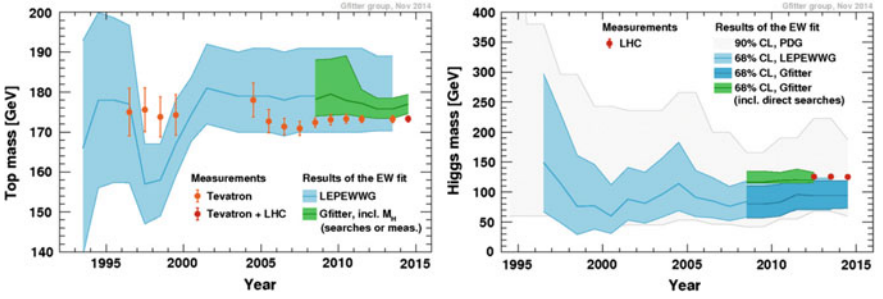

Fig. 7.7 Calculated mass of the top quark (left) and of the Higgs boson (right) from fits of experimental data to the standard model, as function of the year. The lighter bands represent the theoretical predictions at 95% confidence level, while the dark bands at 68% confidence level. The points with error bars represent the experimental values after the discovery of these particles. From http://project-gfitter.web.cern.ch/project-gfitter

Both the mass of the top quark and mass of the Higgs boson were predicted before their discovery (Fig. 7.7), and the masses measured by experiment confirmed the prediction.

Many other consistency tests at accelerators confirmed the validity of the standard model; we shall discuss them in the next section.

7.5 Experimental Tests of the Standard Model at Accelerators

The SM has been widely tested, also in the cosmological regime, and with high-precision table-top experiments at sub-GeV energies. The bulk of the tests, however, has been performed at particle accelerators, which span a wide range of high energies.

In particular, from 1989 to 1995, the large electron–positron collider (LEP) at CERN provided collisions at center-of-mass energies near the Z mass; four large state-of-the-art detectors (ALEPH, DELPHI, L3, and OPAL) recorded about 17 million Z decays. Almost at the same time, the SLD experiment at the SLAC laboratory near Stanford, California, collected 600 000 Z events at the SLAC Linear Collider (SLC), with the added advantage of a longitudinally polarized electron beam—polarization provided additional opportunities to test the SM. LEP was upgraded later to higher energies starting from 1996 and eventually topped at a center-of-mass energy of about 210 GeV at the end of 2000. In this second phase, LEP could produce and study at a good rate of all SM particles—except the top quark and the Higgs boson; it produced in particular a huge statistics of pairs of W and Z bosons.

The Tevatron circular accelerator at the Fermilab near Chicago collided protons and antiprotons in a 7-km ring to energies of up to 1 TeV. It was completed in 1983, and its main achievement was the discovery of the top quark in 1995 by the scientists of the CDF and D0 detectors. The Tevatron ceased operations in 2011 because of the completion of the LHC, which had started stable operations in early 2010.

Finally, the Large Hadron Collider (LHC) was built in the 27 km long LEP tunnel; it collides pairs of protons (and sometimes of heavy ions). It started stable operation in 2010 and increased, in 2015, its center-of-mass energy to 13 TeV for proton–proton collisions. Its main result has been the discovery of the Higgs boson.

All these accelerators provided extensive tests of the standard model; we shall review them in this section.

Before summarizing the main SM results at LEP/SLC, at the Tevatron and at the LHC, let us shortly remind some of the earlier results at accelerators which gave the scientific community confidence in the electroweak part of the standard model and were already presented in Chap. 6:

- The discovery of the weak neutral currents by Gargamelle in 1972. A key prediction of the electroweak model was the existence of neutral currents mediated by the Z. These currents are normally difficult to reveal, since they are hidden by the most

probable photon interactions. However, the reactions

$$\bar{\nu}_\mu + e^- \to \bar{\nu}_\mu + e^- \quad ; \quad \nu_\mu + N \to \nu_\mu + X$$

cannot happen via photon exchange, nor via W exchange. The experimental discovery of these reactions happened in bubble-chamber events, thanks to Gargamelle, a giant bubble chamber. With a length of 4.8 m and a diameter of nearly 2 m, Gargamelle held nearly 12 m^3 of liquid freon and operated from 1970 to 1978 with a muon neutrino beam produced by the CERN Proton Synchrotron. The first neutral current event was observed in December 1972, and the detection was published with larger statistics in 1973; in the end, approximately 83,000 neutrino interactions were analyzed, and 102 neutral current events observed. Gargamelle is now on exhibition in the CERN garden.

- The discovery of a particle made of the charm quark (the J/ψ) in 1974. Charm was essential to explain the absence of strangeness-changing neutral currents (by the so-called GIM mechanism, discussed in the previous chapter).
- The discovery of the W and Z bosons at the CERN $Sp\bar{p}S$ collider in 1983, in the mass range predicted, and consistent with the relation $m_Z \simeq m_W / \cos\theta_W$.

7.5.1 Data Versus Experiments: LEP (and the Tevatron)

LEP has studied all the SM particles, except the top and the Higgs, which could not be produced since the c.m. energy was not large enough. Most of the results on the SM parameters are thus due to LEP. We shall see, however, that Tevatron and the LHC are also crucial for the test of the SM.

7.5.1.1 Electroweak Precision Measurements

In the context of the Minimal Standard Model (MSM) neglecting the neutrino masses which are anyway very small, electroweak processes can be computed at tree level from the electromagnetic coupling α, the weak coupling G_F, the Z mass M_Z, and from the elements of the CKM mixing matrix.

When higher-order corrections and phase space effect are included, one has to add to the above α_s, m_H, and the masses of the particles. The calculations show that the loops affecting the observables depend on the top mass through terms (m_t^2/M_Z^2), and on the Higgs mass through terms showing a logarithmic dependence $\ln(m_H^2/M_Z^2)$—plus, of course, on any kind of "heavy new physics" (see Sect. 7.4).

The set of the three SM variables which characterize the interaction is normally taken as $M_Z = 91.1876 \pm 0.0021$ GeV (derived from the Z line shape, see later), $G_F = 1.1663787(6) \times 10^5$ GeV^{-2} (derived from the muon lifetime), and the fine structure constant in the low-energy limit $\alpha = 1/137.035999074(44)$, taken from

several electromagnetic observables; these quantities have the smallest experimental errors.

One can measure the SM parameters through thousands of observables, with partially correlated statistical and systematic uncertainties; redundancy can display possible contradictions, pointing to new physics. This large set of results has been reduced to a more manageable set of 17 precision results, called electroweak observables. This was achieved by a model-independent procedure, developed by the LEP and Tevatron Electroweak Working Groups (a group of physicist from all around the world charged of producing "official" fits to precision observables in the SM).

About three-fourth of all observables arise from measurements performed in electron–positron collisions at the Z resonance, by the LEP experiments ALEPH, DELPHI, L3, and OPAL, and the SLD experiment. The Z-pole observables are five observables describing the Z lineshape and leptonic forward–backward asymmetries, two observables describing polarized leptonic asymmetries measured by SLD with polarized beams and at LEP through the tau polarization, six observables describing b and $c$quark production at the Z pole, and finally the inclusive hadronic charge asymmetry. The remaining observables are the mass and total width of the W boson measured at LEP and at hadron accelerators, the top quark mass measured at hadron accelerators. Recently, also the Higgs mass has been added to the list; the fact that the Higgs mass has been found in the mass range predicted by the electroweak observables is another success of the theory.

Figure 7.8 shows the comparison of the electroweak observables with the best fit to the SM. One can appreciate the fact that the deviations from the fitted values are consistent with statistical fluctuations.

Figure 7.9 shows the evolution of the hadronic cross section $\sigma(e^+e^- \to hadrons)$ with energy, compared with the predictions of the SM. This is an incredible success of the SM, which quantitatively accounts for experimental data over a wide range of energies:

- starting from a region (above the Υ threshold and below some 50 GeV) where the production is basically due to photon exchange, and $\sigma \propto 1/s$,
- to a region in which the contributions from Z and γ are important and the Z/γ interference has to be taken into account,
- to a region of Z dominance (Eq. 7.92), and
- to a region in which the WW channel opens and triple boson vertices become relevant.

We describe in larger detail three of the most significant electroweak tests at LEP in phase I: the partial widths of the Z, the forward–backward asymmetries, and the study of the Z line shape, which has important cosmological implications. Finally, in this section, we examine the characteristics of vertices involving three gauge bosons.

Partial Widths of the Z. The partial widths of the Z, possibly normalized to the total width, are nontrivial parameters of the SM. Indeed, the evolution of the branching fractions with energy due to the varying relative weights of the Z and γ couplings is a probe into the theory.

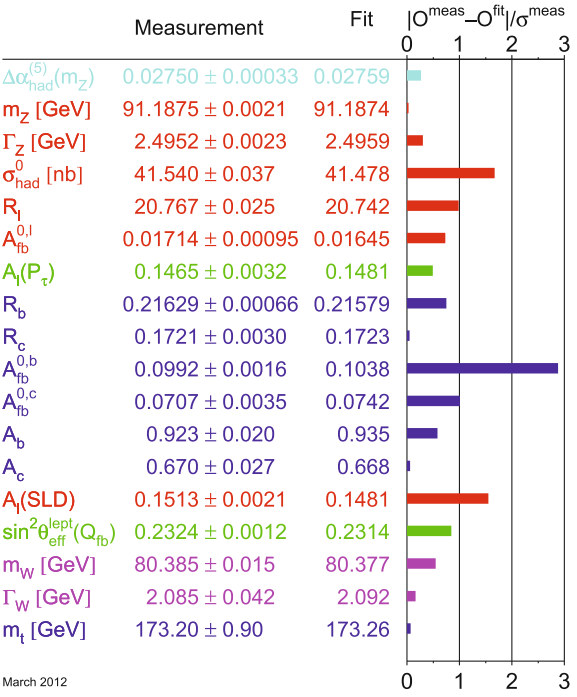

Fig. 7.8 Pull comparison of the fit results with the direct measurements in units of the experimental uncertainty. The absolute value of the pull (i.e., of the difference between the measured value and the fitted value divided by the uncertainty) of the Higgs mass is 0.0 (its value is completely consistent with the theoretical fit)

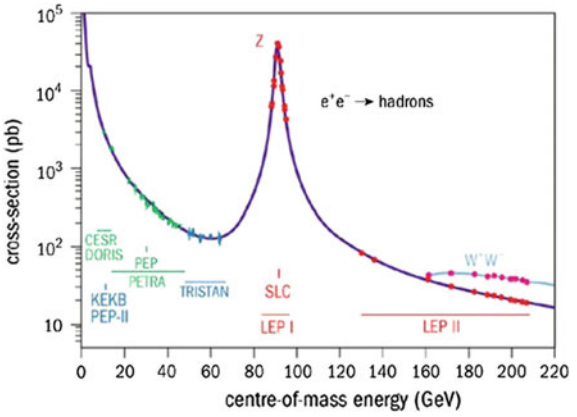

Fig. 7.9 Evolution of the hadronic cross section $\sigma(e^+e^- \to hadrons)$ with energy, compared with the predictions of the SM

Final states of the Z into $\mu^+\mu^-$ and $\tau^+\tau^-$ pairs can easily be identified. The e^+e^- final state is also easy to recognize, but in this case, the theoretical interpretation is less trivial, being the process dominated by $t-$channel exchange at low angles. Among hadronic final states, the $b\bar{b}$ and $c\bar{c}$ can be tagged using the finite lifetimes of the primary hadrons (the typical lifetime of particles containing c quarks and weakly decaying is of the order of 0.1 ps, while the typical lifetime of particles containing b quarks and weakly decaying is of the order of 1 ps). The tagging of $s\bar{s}$ final states is more difficult and affected by larger uncertainties.

All these measurements gave results consistent with the predictions from the SM (Table 7.1). By considering that the decay rates include the square of these factors, and all possible diagrams, the relative strengths of each coupling can be estimated (e.g., sum over quark families and left and right contributions). As we are considering only tree-level diagrams in the electroweak theory, this is naturally only an estimate.

Also, the energy evolution of the partial widths from lower energies and near the Z resonance is in agreement with the Z/γ mixing in the SM.

Z Asymmetries and $\sin^2\theta_{\text{eff}}$. Like the cross section $Z \to f\bar{f}$, the forward–backward asymmetry

$$A_{\text{FB}}^{f} \equiv \frac{\sigma_F - \sigma_B}{\sigma_F + \sigma_B} \simeq \frac{3}{4} A_e A_f \,, \tag{7.90}$$

where F (forward) means along the e^- direction, where the combinations A_f are given, in terms of the vector and axial vector couplings of the fermion f to the Z boson, by

$$A_f = \frac{2 g_V^f g_A^f}{g_V^{f2} + g_A^{f2}} \,, \tag{7.91}$$

can be measured for all charged lepton flavors, for heavy quarks, with smaller accuracy for $s\bar{s}$ pairs, and for all five quark flavors inclusively (overall hadronic asymmetry). It thus allows a powerful test of the SM.

One thus expects at the Z asymmetry values of about 7% for up-type quarks, about 10% for down-type quarks, and about 2% for leptons. Figure 7.8 shows that results are consistent with the SM predictions, being the largest deviation (3 standard deviations) on the forward-backward asymmetry of b quark. This observable is powerful in constraining the value of $\sin\theta_W$ (Fig. 7.10).

Table 7.1 Relative branching fractions of the Z into $f\bar{f}$ pairs: predictions at leading order from the SM (for $\sin^2\theta_W = 0.23$) are compared to experimental results

Particle	g_V	g_A	Predicted (%)	Experimental (%)
Neutrinos (all)	1/4	1/4	20.5	(20.00 ± 0.06)
Charged leptons (all)			10.2	(10.097 ± 0.003)
Electron	$-1/4 + \sin^2\theta_W$	$-1/4$	3.4	(3.363 ± 0.004)
Muon	$-1/4 + \sin^2\theta_W$	$-1/4$	3.4	(3.366 ± 0.007)
Tau	$-1/4 + \sin^2\theta_W$	$-1/4$	3.4	(3.367 ± 0.008)
Hadrons (all)			69.2	(69.91 ± 0.06)
Down-type quarks d, s, b	$-1/4 + 1/3$ $\sin^2\theta_W$	$-1/4$	15.2	(15.6 ± 0.4)
Up-type quarks u, c	$1/4 - 2/3 \sin^2\theta_W$	1/4	11.8	(11.6 ± 0.6)

Since the e^+e^- annihilation as a function of energy scans the γ/Z mixing, the study of the forward–backward asymmetry as a function of energy is also very important. The energy evolution of the asymmetries from lower energies and near the Z resonance is in agreement with the Z/γ mixing in the SM.

The Z Lineshape and the Number of Light Neutrino Species. One of the most important measurements at LEP concerns the mass and width of the Z boson. While the Z mass is normally taken as an input to the standard model, its width depends on the number of kinematically available decay channels and the number of light neutrino species (Fig. 7.11). As we shall see, this is both a precision measurement confirming the SM and the measurement of a fundamental parameter for the evolution of the Universe.

Why is the number of quark and lepton families equal to three? Many families including heavy charged quarks and leptons could exist, without these heavy leptons being ever produced in accessible experiments, because of a lack of energy. It might be, however, that these yet undiscovered families include "light" neutrinos, kinematically accessible in Z decays—and we might see a proof of their existence in Z decays. The Z lineshape indeed obviously depends on the number of *kinematically accessible* neutrinos. Let us call them "light" neutrinos.

Around the Z pole, the $e^+e^- \to Z \to f\bar{f}$ annihilation cross section (s-channel) can be written as

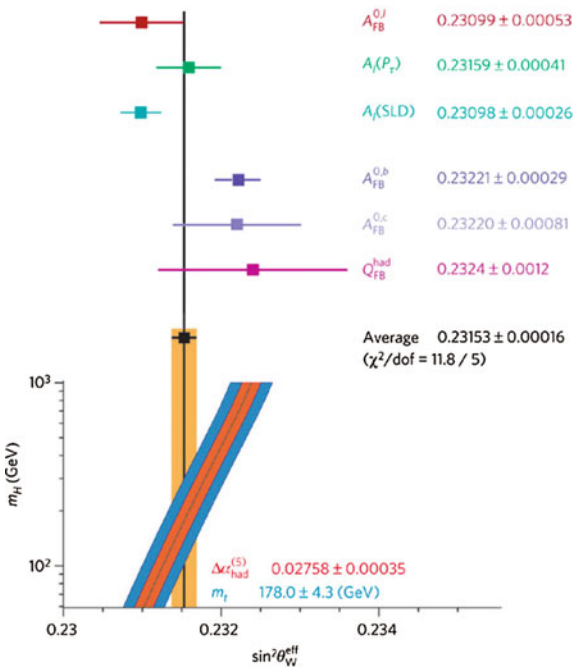

Fig. 7.10 Comparison of the effective electroweak mixing angle $\sin^2\theta_{\text{eff}}^{\text{lept}}$ derived from measurements depending on lepton couplings only (top) and on quark couplings as well (bottom). Also shown is the standard model prediction as a function of the Higgs mass, m_H. From M. Grunewald, CERN Courier, November 2005

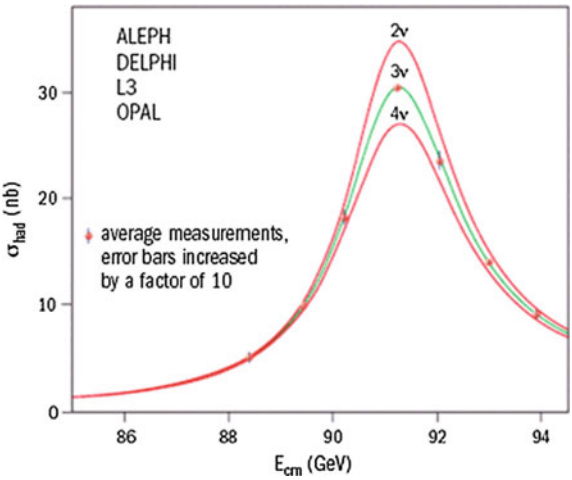

Fig. 7.11 Measurements of the hadron production cross section around the Z. The curves indicate the predicted cross section for two, three, and four neutrino species with standard model couplings and negligible mass. From M. Grunewald, CERN Courier, November 2005

$$\sigma_{s,Z} \simeq \frac{12\pi(\hbar c)^2}{M_Z^2} \frac{s\Gamma_e\Gamma_f}{(s-M_Z^2)^2 + s^2\Gamma_Z^2/M_Z^2} + \text{corrections}. \tag{7.92}$$

The term explicitly written is the generic cross section for the production of a spin one particle in an e^+e^- annihilation, decaying into visible fermionic channels—just a particular case of the Breit–Wigner shape. The peak sits around the Z mass and has a width Γ_Z. $B_f\Gamma_Z = \Gamma_f$ is the partial width of the Z into $f\bar{f}$. As we have seen, the branching fraction of the Z into hadrons is about 70%, each of the leptons represents 3%, while three neutrinos would contribute for approximately a 20%. The term "corrections" includes radiative corrections and the effects of the presence of the photon. We remind that the branching fractions of the photon are proportional to Q_f^2, where Q_f is the electric charge of the final state. However, at the peak, the total electromagnetic cross section is less than 1% of the cross section at the Z resonance. Radiative corrections, instead, are as large as 30%; due to the availability of calculations up to second order in perturbation theory, this effect can be corrected for with a relative precision at the level of 10^{-4}. The effect of a number of neutrinos larger than three on the formula (7.92) would be to increase the width and to decrease the cross section at the resonance.

The technique for the precision measurement of the Z cross section near the peak is not trivial; we shall just sketch it here. The energy of the beam, accurately determined from the measurement of the precession frequencies of the spins of the electron and positron beams, is varied in small steps, and all visible final states channels are classified according to four categories: hadrons, electron pairs, muon pairs, and tau pairs. The extraction of the cross section from the number of events implies the knowledge of the luminosity of the accelerator. This is done by measuring at the same time another process with a calculable cross section, the elastic scattering $e^+e^- \to e^+e^-$ in the $t-$channel (Bhabha scattering, see Chap. 6), which results in an electron–positron pair at small angle. Of course one has to separate this process from

the s-channel, and a different dependence on the polar angle is used for this purpose: the Bhabha cross section depends on the polar angle as $1/\sin^3\theta$, and quickly goes to 0 as θ grows. Another tool can be leptons universality: in the limit in which the lepton masses are negligible compared to the Z mass, the branching fractions of all leptons are equal.

In the end, one has a measurement of the total hadronic cross section from the LEP experiments (with the SLAC experiments contributing to a smaller extent due to the lower statistics) which is plotted in Fig. 7.11. The best fit to Eq. 7.92, assuming that the coupling of neutrinos is universal, provides

$$N_\nu = 2.9840 \pm 0.0082\,. \tag{7.93}$$

Notice that the number of neutrinos could be fractional—in case a fourth generation is relatively heavy—and universality is apparently violated due to the limited phase space.

The best-fit value of the Z width is

$$\Gamma_Z = 2.4952 \pm 0.0023\,\text{GeV}\,. \tag{7.94}$$

The existence of additional light neutrinos would have considerable cosmological consequences: the evolution of the Universe immediately after the Big Bang would be affected. The creation of neutrons and protons is controlled by reactions involving the electron neutrino, such as $\nu_e\, n \to p\, e$ and is consequently sensitive to the number of light neutrino families N_ν which compete with electron neutrinos. Primordial nucleosynthesis (Sect. 8.1.4) is sensitive to this number.

A Fundamental Test: the WW and ZZ Cross Sections. One of the main scientific goals of the LEP II (i.e., at energies above the Z) program has been the measurement of the triple gauge vertices, through the experimental channels $e^+e^- \to WW$ and $e^+e^- \to ZZ$.

At tree level, the W-pair production process $e^+e^- \to W^+W^-$ involves three different contributions (Fig. 7.12), corresponding to the exchange of ν_e, γ, and Z. If the ZWW vertex would not exist, and the WW production occurred only via the neutrino exchange diagram, the WW production cross section would diverge for large values of $\sqrt{s}$. As shown in Fig. 7.13, the existence of the ZWW vertex is

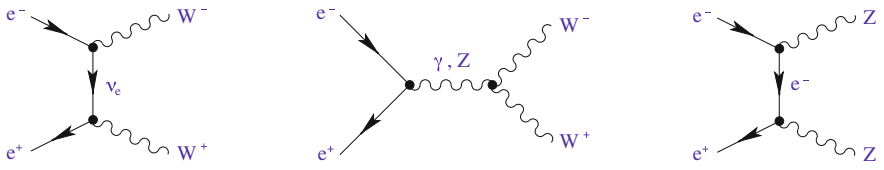

Fig. 7.12 Feynman diagrams contributing to $e^+e^- \to W^+W^-$ and $e^+e^- \to ZZ$

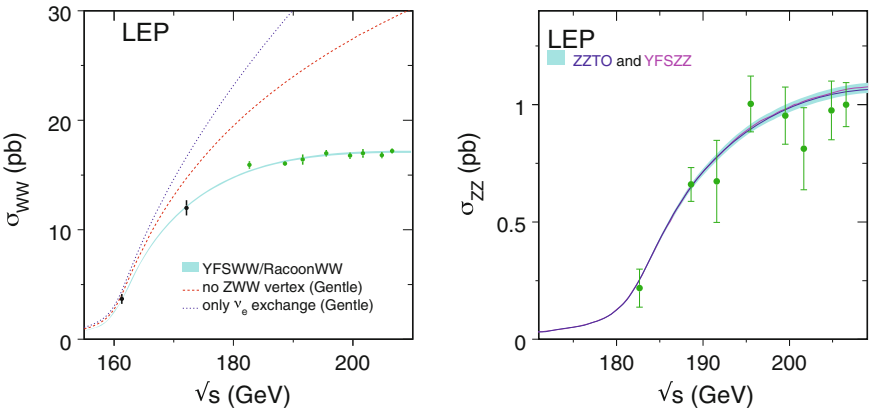

Fig. 7.13 Measured energy dependence of $\sigma(e^+e^- \to W^+W^-)$ (left) and $\sigma(e^+e^- \to ZZ)$ (right). The curves shown for the W-pair production cross section correspond to only the ν_e-exchange contribution (upmost curve), ν_e exchange plus photon exchange (middle curve), and all contributions including also the ZWW vertex (lowest curve). Only the e-exchange mechanism contributes to Z-pair production. From ALEPH, DELPHI, L3, OPAL Collaborations and the LEP Electroweak Working Group, Phys. Rep. 532 (2013) 119

crucial in order to explain the data. At very high energies, the vertex HW^+W^- is also needed to prevent the divergence of the cross section.

Since the Z does not interact with the photon as it is electrically neutral, the SM does not include any local γZZ vertex. This leads to a $e^+e^- \to ZZ$ cross section that involves only the contribution from e exchange.

The agreement of the SM predictions with the experimental measurements in both production channels, W^+W^- and ZZ, is an important test for the gauge self-interactions. There is a clear signal of the presence of a ZWW vertex, with the predicted strength. Moreover, there is no evidence for any γZZ or ZZZ interactions. The gauge structure of the $\mathrm{SU}(2)_L \otimes \mathrm{U}(1)_Y$ theory is nicely confirmed by the data.

The experimental data at LEP II and at hadronic accelerators (mostly the Tevatron) have allowed the determination of the W mass and width with high accuracy:

$$M_W = 80.385 \pm 0.015\,\mathrm{GeV} \tag{7.95}$$

$$\Gamma_W = 2.085 \pm 0.042\,\mathrm{GeV}\,. \tag{7.96}$$

7.5.1.2 QCD Tests at LEP

After our considerations on the electroweak observables, let us now summarize the tests of the remaining building block of the SM: QCD.

LEP is an ideal laboratory for QCD studies since the center-of-mass energy is high with respect to the masses of the accessible quarks and (apart from radiative corrections which are important above the Z) well defined. As a consequence of the

large center-of-mass energy, jets are collimated and their environment is clean: the hadron level is not so far from the parton level. The large statistics collected allows investigating rare topologies.

In particular, LEP confirmed the predictions of QCD in the following sectors—among others:

- QCD is not Abelian: the jet topology is inconsistent with an Abelian theory and evidences the existence of the three-gluon vertex.
  Angular correlations within four-jet events are sensitive to the existence of the gluon self-coupling (Fig. 7.14) and were extensively studied at LEP.
  As a consequence of the different couplings in the $gq\bar{q}$ and ggg vertices, the distribution of the Bengtsson–Zerwas angle (Fig. 7.15, left) between the cross product of the direction of the two most energetic jets in four-jet events and the

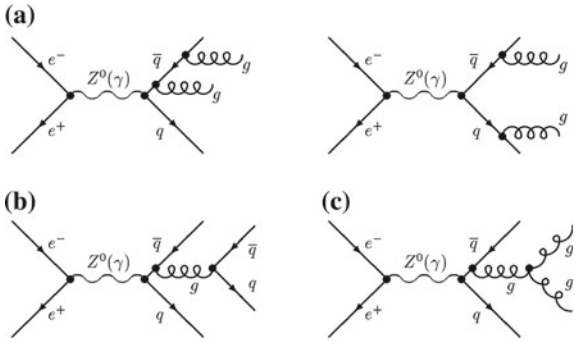

Fig. 7.14 Diagrams yielding four-parton final states **a** double gluon bremsstrahlung; **b** secondary $q\bar{q}$ pair production; **c** triple-gluon vertex

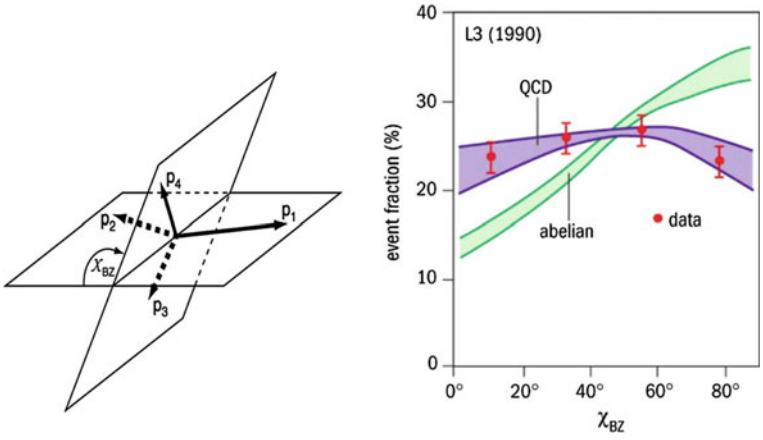

Fig. 7.15 Left: Definition of the Bengtsson–Zerwas angle in four-jet events. From P.N. Burrows, SLAC-PUB-7434, March 1997. Right: Distribution for the data, compared with the predictions for QCD and for an Abelian theory. The experimental distribution is compatible with QCD, but it cannot be reproduced by an Abelian field theory of the strong interactions without gauge boson self-coupling. From CERN Courier, May 2004

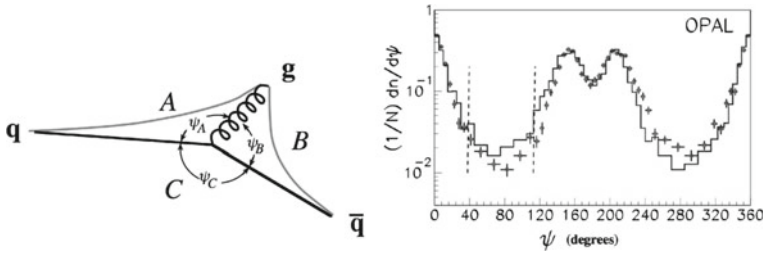

Fig. 7.16 Left: Sketch of a three-jet event in e^+e^- annihilations. In the Lund string model for fragmentation, string segments span the region between the quark q and the gluon g and between the antiquark $\bar{q}$ and the gluon. Right: Experimental measurement of the particle flow $(1/N)dn/d\psi$, for events with $\psi_A = 150° \pm 10°$ and $\psi_C = 150° \pm 10°$. The points with errors show the flow from the higher energy quark jet to the low-energy quark jet and then to the gluon jet; in the histogram, it is shown the measured particle flow for the same events, starting at the high-energy quark jet but proceeding in the opposite sense. The dashed lines show the regions, almost free of the fragmentation uncertainties, where the effect is visible. From OPAL Collaboration, Phys. Lett. B261 (1991) 334

cross product of the direction of the two least energetic jets is substantially different in the predictions of QCD and of an Abelian theory where the gluon self-coupling does not exist.

The LEP result is summarized in Fig. 7.15, right; they are in excellent agreement with the gauge structure of QCD and proved to be inconsistent with an Abelian theory; i.e., the three-gluon vertex is needed to explain the data.

- Structure of QCD: measurement of the color factors.

  QCD predicts that quarks and gluons fragment differently due to their different color charges. Gluon jets are expected to be broader than quark jets; the multiplicity of hadrons in gluon jets should be larger than in quark jets of the same energy, and particles in gluon jets are expected to be less energetic. All these properties have been verified in the study of symmetric three-jet events, in which the angle between pairs of consecutive jets is close to 120°—the so-called Mercedes events, like the event in Fig. 6.61, right. In these three-jet events, samples of almost pure gluon jets could be selected by requiring the presence of a particle containing the b quark in both the other jets—this can be done due to the relatively long lifetime associated to the decay ($\tau_b \simeq 1$ ps, which corresponds to an average decay length of 300 μm for $\gamma = 1$, well measurable, for example, with Silicon vertex detectors). Many observables at hadron level can be computed in QCD using the so-called local parton-hadron duality (LPHD) hypothesis, i.e., computing quantities at parton level with a cutoff corresponding to a mass just above the pion mass and then rescaling to hadrons with a normalization factor.

  Gluon jets in hadronic three-jet events at LEP have indeed been found experimentally to have larger hadron multiplicities than quark jets. Once correcting for hadronization effects, one obtains

$$\frac{C_A}{C_F} = 2.29 \pm 0.09\,(\text{stat.}) \pm 0.15(\text{theory})\,,$$

consistent with the ratio of the color factors $C_A/C_F = 9/4$ that one can derive from the theory at leading order assuming LPHD (see Eq. 6.332).

- String effect.
  As anticipated in Sect. 6.4.6 and as one can see from Fig. 7.16, left, one expects in a Mercedes event an excess of particles in the direction of the gluon jet with respect to the opposite direction, since this is where most of the color field is. This effect is called the string effect and has been observed by the LEP experiments at CERN in the 1990s. This is evident also from the comparison of the color factors, as well as from considerations based on color conservation.
  A direct measurement of the string effect in Mercedes events is shown in Fig. 7.16, right.
- Measurement of α_s and check of its evolution with energy.
  One of the theoretically best known variables depending on α_s is the ratio of the Z partial decay widths R^0_{lept}, which is known to $\mathcal{O}(\alpha_s^3)$:

$$R^0_{\text{lept}} = \frac{\Gamma_{\text{hadrons}}}{\Gamma_{\text{leptons}}} = 19.934 \left[1 + 1.045 \left(\frac{\alpha_s}{\pi}\right) + 0.94 \left(\frac{\alpha_s}{\pi}\right)^2 - 15 \left(\frac{\alpha_s}{\pi}\right)^3\right] + \mathcal{O}\left(\frac{\alpha_s}{\pi}\right)^4 . \tag{7.97}$$

From the best-fit value $R^0_{\text{lept}} = 20.767 \pm 0.025$ (derived by assuming lepton universality), one obtains

$$\alpha_s(m_Z) = 0.124 \pm 0.004(\text{exp.}) \, {}^{+0.003}_{-0.002}(\text{theory}). \tag{7.98}$$

The advantage of evaluating α_s from Eq. 7.97 is that nonperturbative corrections are suppressed since this quantity does not depend on hadronization, and the dependence on the renormalization scale μ is small. This renormalization scale is often responsible for the dominant uncertainty of α_s measurements. A fit to all electroweak Z pole data from LEP, SLD and to the direct measurements of m_t and m_W leads to

$$\alpha_s(m_Z) = 0.1183 \pm 0.0027. \tag{7.99}$$

One could ask if these are the most reliable evaluations of $\alpha_s(m_Z)$ using the LEP data. The problem is that the quoted results depend on the validity of the electroweak sector of the SM, and thus small deviations can lead to large changes. One can also measure α_s from infrared safe hadronic event shape variables like jet rates, etc., not depending on the electroweak theory. A fit to the combined data results in a value

$$\alpha_s(m_Z) = 0.1195 \pm 0.0047,$$

where the error is almost entirely due to theoretical uncertainties (renormalization scale effects). The consistency of this value with the result in Eq. 7.99 is in itself a confirmation of QCD. Measurements of α_s at LEP energies using a multitude of analysis methods are collected in Fig. 7.17; one can appreciate their consistency.

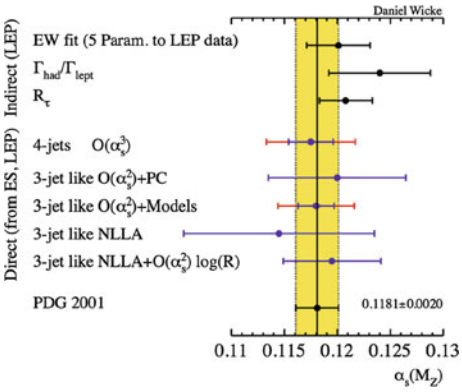

Fig. 7.17 Summary of α_s measurements at LEP compared to the world average. The theoretical uncertainty for all five measurements from event shapes (ES) is evaluated by changing the renormalization scale μ by a factor of 2

- Nonperturbative QCD: evolution of average charge multiplicity with center-of-mass energy.
  As already seen in Chap. 6, average multiplicity is one of the basic observables characterizing hadronic final states; experimentally, since the detection of charged particles is simpler than the detection of neutrals, one studies the average charged particle multiplicity. In the limit of large energies, most of the particles in the final state are pions, and one can assume, by isospin symmetry, that the number of neutral pions is half the number of charged pions.
  LEP in particular has studied multiplicity of charged particles with lifetimes larger than 1 ps in a wide range of energies; using radiative events (i.e., events $e^+e^- \to Z'\gamma$ where the Z' is off-shell with respect to the Z), one could obtain, thanks to the large statistics collected at LEP in phase I, information also on the behavior of this observable at center-of-mass energies below the Z peak.
  The QCD prediction including leading and next-to-leading order calculation is

$$\langle n \rangle (E_{\mathrm{CM}}) = a[\alpha_s(E_{\mathrm{CM}})]^b e^{c/\sqrt{\alpha_s(E_{\mathrm{CM}})}} \left[1 + \mathcal{O}(\sqrt{\alpha_s(E_{\mathrm{CM}})}\right] , \qquad (7.100)$$

  where a is the LPHD scaling parameter (not calculable from perturbation theory) whose value should be fitted from the data; the constants $b = 0.49$ and $c = 2.27$ are instead calculated from the theory. The summary of the experimental data available is shown in Fig. 7.18 with the best fit to the QCD prediction.
  Energy distribution of hadrons can be computed form LPHD; the coherence between radiated gluons causes a suppression at low energies. Experimental evidence for this phenomenon comes from the "hump-backed" plateau of the distribution of the variable $\xi = -\ln(2E_h/E_{\mathrm{CM}})$ shown in Fig. 7.19, left.
  The increase with energy of the maximum value, ξ^*, of these spectra is strongly reduced compared to expectations based on phase space (Fig. 7.19, right).

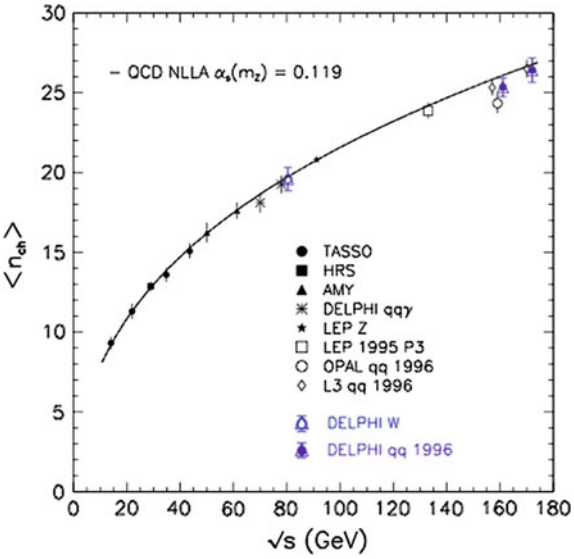

Fig. 7.18 Measured average charged particle multiplicity in $e^+e^- \to q\bar{q}$ events as a function of center-of-mass energy $\sqrt{s}$. DELPHI high-energy results are compared with other experiments and with a fit to the prediction from QCD in next-to-leading order. The average charged particle multiplicity in W decays is also shown at an energy corresponding to the W mass. The measurements have been corrected for the different proportions of $b\bar{b}$ and $c\bar{c}$ events at the various energies

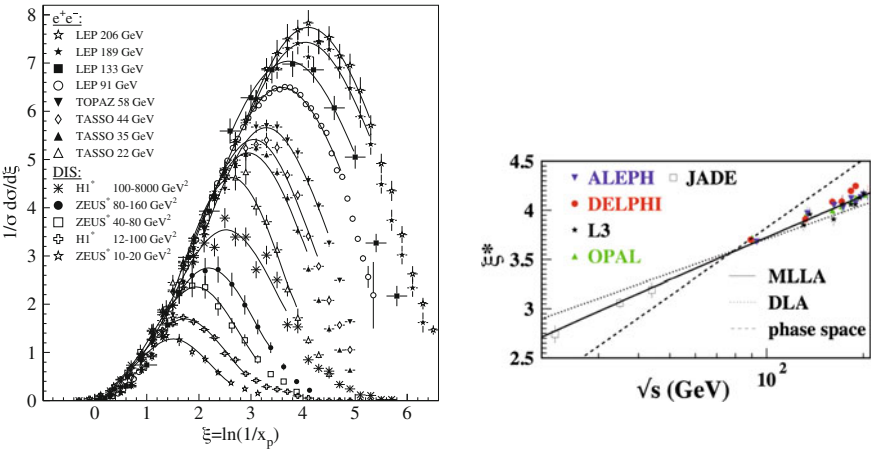

Fig. 7.19 Left: Center-of-mass energy dependence of the spectra of charged hadrons as a function of $\xi = -\ln x$; $x = 2E_h/E_{\mathrm{CM}}$. From K.A. Olive et al. (Particle Data Group), Chin. Phys. C 38 (2014) 090001. Right: Energy dependence of the maximum of the ξ distribution, ξ^*

7.5.1.3 The Discovery of the Top Quark at the "Right" Mass at the Tevatron

LEP could not discover the top quark but was able to indirectly estimate its mass, since the top quark mass enters into calculations of characteristics of various electroweak observables, as seen before.

In 1994, the best (indirect) estimate for the top quark mass by LEP was $m_t = 178 \pm 20\,\text{GeV}$.

In March 1995, the two experiments CDF and D0 running at Fermilab at a center-of-mass energy of 1.8 TeV jointly reported the discovery of the top at a mass of $176 \pm 18\,\text{GeV}$. The cross section was consistent with what predicted by the standard model. Figure 7.7, left, compares the indirect measurements of the top mass with the direct measurements.

7.5.2 LHC and the Discovery of the Higgs Boson

Despite the incredible success on the precision measurements related to standard model properties, LEP just missed one of its most important targets: the discovery of the Higgs boson. Indeed there was a hot debate at CERN on the opportunity to increase the LEP c.m. energy up to 220 GeV by installing more super-conducting RF cavities; the final decision was negative and the Higgs particle was found more than a decade after the LEP shutdown, thanks to the LHC proton–proton collider.

7.5.2.1 The Legacy of Indirect Measurements and Previous Unsuccessful Searches

The most important processes which could possibly produce a Higgs boson at LEP were, besides the unobserved decays $Z \to H + \gamma$ or $Z \to H + Z^*(Z^* \to f\bar{f})$, (a) the so-called Higgs-strahlung $e^+e^- \to Z + H$; and (b) the vector boson (W^+W^- or ZZ) fusion into a H boson and a lepton–antilepton pair (Fig. 7.20). The direct process $e^+e^- \to H$ as a negligible probability because of the small H coupling to e^+e^-, given the small value of the mass of the electron.

A first limit on the Higgs mass was obtained shortly after switching on the accelerator: the fact that no decays of the Z into H were observed immediately implies that the Higgs boson must be heavier than half the mass of the Z. Then the center-of-mass energy of LEP was increased up to 210 GeV, still without finding evidence for the Higgs. Indirect experimental bounds on the SM Higgs boson mass (in the hypothesis of a minimal SM) were obtained from a global fit of precision measurements of electroweak observables at LEP described in the previous subsection; the uncertainty on radiative corrections was dominated by the uncertainty on the yet undiscovered Higgs boson—and, to a smaller extent, by the error on the measurement of the top mass: solid bounds could thus be derived.

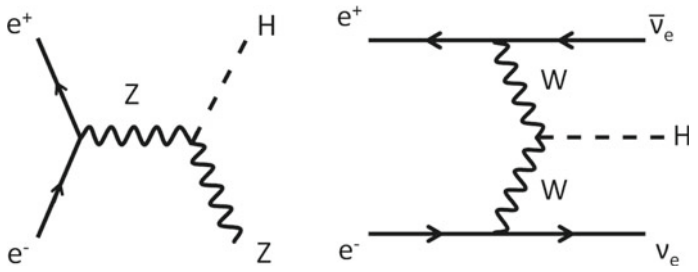

Fig. 7.20 Main Higgs production mechanisms at LEP: Higgs-strahlung (left) and vector boson fusion (right)

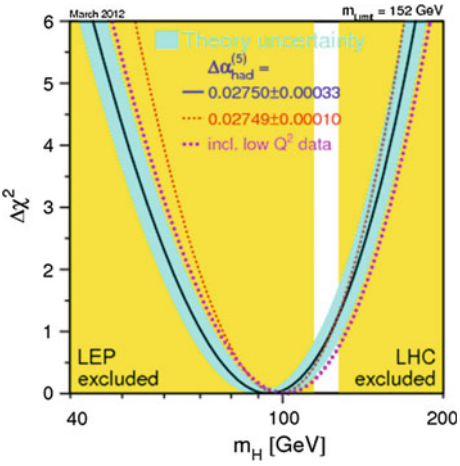

Fig. 7.21 Probability distribution for the mass of the Higgs boson before its direct discovery: fit to the standard model. Fit from the electroweak working group

LEP shut down in the year 2000. The global fit to the LEP data, with the constraints given by the top mass measurements at the Tevatron, suggested for the Higgs a mass of 94^{+29}_{-24} GeV (the likelihood distribution was peaked toward lower Higgs mass values, as shown in Fig. 7.21). On the other hand, direct searches for the Higgs boson conducted by the experiments at the LEP yielded a lower limit at 95% C.L. (confidence limit)

$$m_H > 114.4\,\text{GeV}\,. \tag{7.101}$$

Higgs masses above 171 GeV were also excluded at 95% C.L. by the global electroweak fit. The negative result of searches at the Tevatron and at LHC conducted before 2011 excluded the range between 156 and 177 GeV; thus one could conclude, still at 95% C.L.,

$$m_H < 156\,\text{GeV}\,. \tag{7.102}$$

Scientists were finally closing on the most wanted particle in the history of high-energy physics.

7.5.2.2 LHC and the Higgs

The Large Hadron Collider at CERN, LHC, started operation in September 2008 for a test run at center-of-mass (c.m.) energy smaller than 1 TeV and then in a stable conditions in November 2009 after a serious accident in the test run damaged the vacuum tubes and part of the magnets. Starting from March 2010, LHC reached an energy of 3.5 TeV per beam, and thus an excellent discovery potential for the Higgs; the energy was further increased to 4 TeV per beam in mid 2012. This phase, called "Run 1," lasted till February 2013, when LHC was shut down for a two-year upgrade, meant to allow collisions at energies up 14 TeV in the c.m. In April 2015, the LHC restarted operations (Run 2), with the magnets handling 6.5 TeV per beam (13 TeV total). The total number of collisions in 2016 exceeded the number from Run 1 and was even higher in 2017.

Within the strict bound defined by (7.101) and (7.102), a mass interval between 120 and 130 GeV was highly probable for the Higgs when LHC started operating. A Higgs particle around that mass range is mostly produced at LHC (Fig. 7.22) via:

- gluon–gluon fusion (gluon–gluon fusion can generate a virtual top quark loop, and since the Higgs couples to mass, this process is very effective in producing Higgs bosons, the order of magnitude of the cross section being of 10 pb),
- weak-boson fusion (WBF),
- associated production with a gauge boson,
- associated production with a heavy quark-antiquark pair (or one heavy quark).

The relevant cross sections are plotted in Fig. 7.23, left.

A Higgs particle between 120 and 130 GeV is difficult to detect at the LHC, because the W^+W^- decay channel is kinematically forbidden (one of the Ws has to be highly virtual). The total decay width is about 4 MeV; the branching fractions predicted by the SM are depicted in Fig. 7.23, right. The dominant decay modes are $H \to b\bar{b}$ and $H \to WW^*$. The first one involves the production of jets, which are difficult to separate experimentally in the event; the second one involves jets and/or missing energy (in the semileptonic W, decay part of the energy is carried by an undetected neutrino, which makes the event reconstruction difficult). The decay $H \to ZZ$ might have some nice experimental features: the final state into four light charged leptons is relatively easy to separate from the background. The decay $H \to \gamma\gamma$, although suppressed at the per mil level, has a clear signature; since it happens via a loop, it provides indirect information on the Higgs couplings to WW, ZZ, and $t\bar{t}$.

On July 4, 2012, a press conference at CERN followed worldwide finally announced the observation at the LHC detectors ATLAS and CMS of a narrow resonance with a mass of about 125 GeV, consistent with the SM Higgs boson. The evidence was statistically significant, above five standard deviations in either experiment; decays to $\gamma\gamma$ and to $ZZ \to 4$ leptons were detected, with rates consistent with those predicted for the SM Higgs.

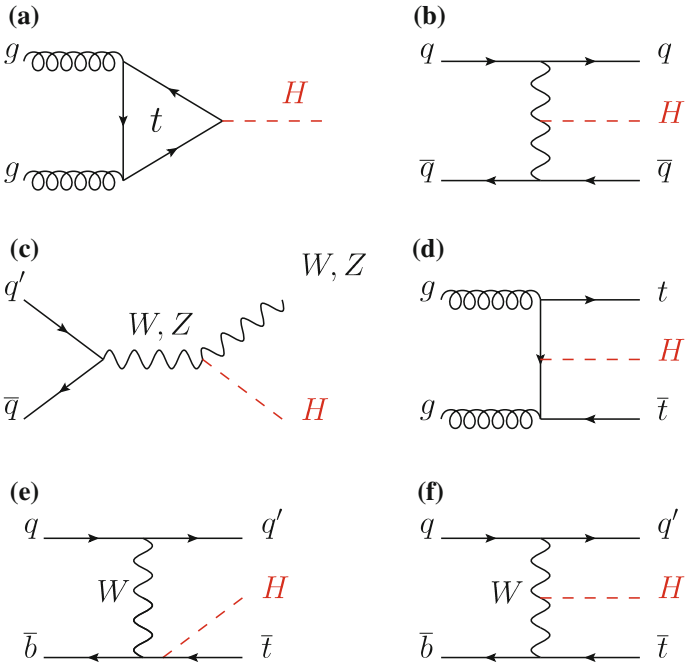

Fig. 7.22 Main leading order Feynman diagrams contributing to the Higgs production in **a** gluon fusion, **b** vector-boson fusion, **c** Higgs-strahlung (or associated production with a gauge boson), **d** associated production with a pair of top (or bottom) quarks, **e–f** production in association with a single top quark

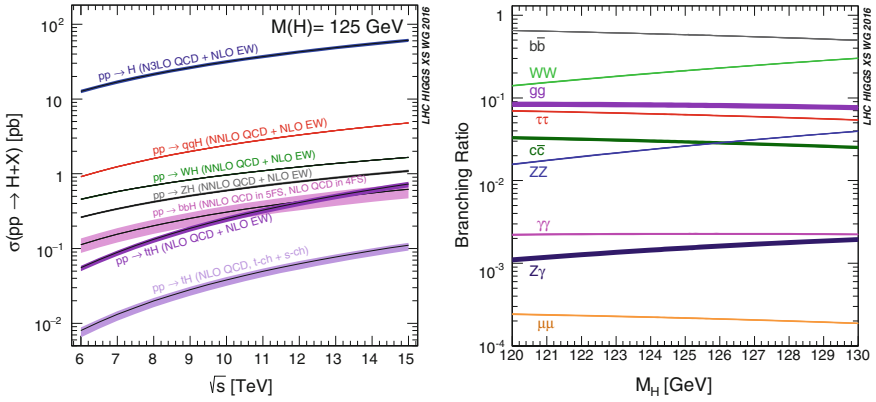

Fig. 7.23 Left: Production cross sections for a SM Higgs boson of mass 125 GeV as a function of the c.m. energy, $\sqrt{s}$, for pp collisions.Right: Branching ratios expected for the decay of a Higgs boson of mass between 120 and 130 GeV. From C. Patrignani et al. (Particle Data Group), Chin. Phys. C, 40, 100001 (2016) and 2017 update

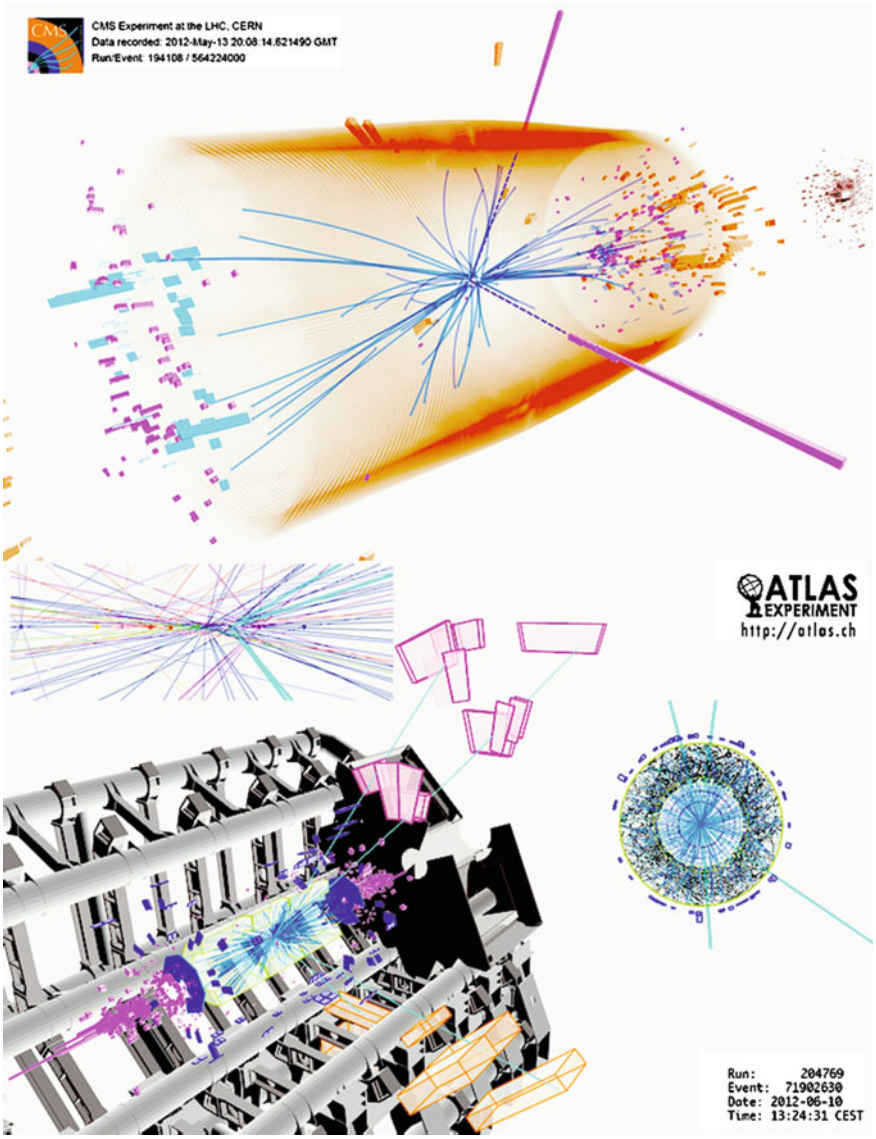

Fig. 7.24 Candidate Higgs boson events at the LHC. The upper panel shows a Higgs decay into two photons (dashed lines and towers) recorded by CMS. The lower panel shows a decay into four muons (thick solid tracks) recorded by ATLAS. Source: CERN

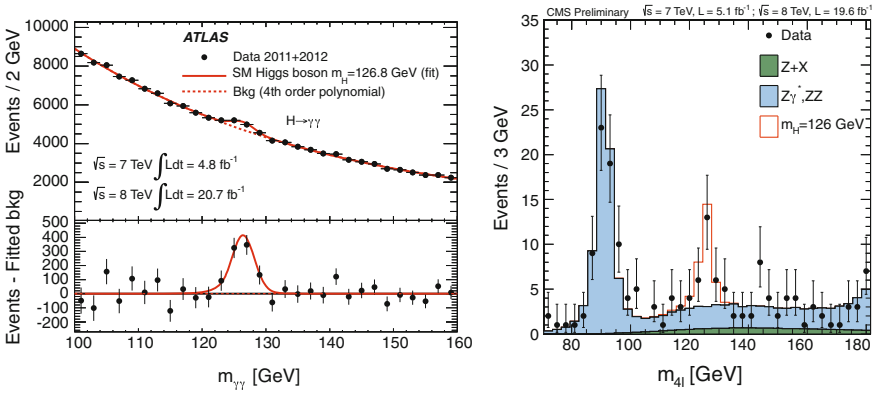

Fig. 7.25 Invariant mass of the $\gamma\gamma$ candidates in the ATLAS experiment (left; in the lower part of the plot the residuals from the fit to the background are shown) and of the four-lepton events in CMS (right; the expected background is indicated by the dark area, including the peak close to the Z mass and coming from $Z\gamma^*$ events). The plots collect data at the time of the announcement of the Higgs discovery. From K.A. Olive et al. (Particle Data Group), Chin. Phys. C 38 (2014) 090001

Two candidate events—we stress the word "candidate"—are shown in Fig. 7.24. Detection involved a statistically significant excess of such events, albeit with an important background from accidental $\gamma\gamma$ or four-lepton events (Fig. 7.25).

The 2013 Nobel Prize in physics was awarded to François Englert and Peter Higgs "for the theoretical discovery of a mechanism that contributes to our understanding of the origin of mass of subatomic particles, and which recently was confirmed through the discovery of the predicted fundamental particle, by the ATLAS and CMS experiments at CERN's Large Hadron Collider."

Later, the statistics increased, and the statistical significance as well; a compilation of the experimental data by the PDG is shown in Fig. 7.26. The present fitted value for the mass is

$$m_H = 125.09 \pm 0.24\,\mathrm{GeV}/c^2\,, \tag{7.103}$$

consistent with the bounds (7.101) and (7.102).

The discovery of the Higgs was of enormous resonance. First of all, it concluded a 50-year long search based on a theoretical prediction. Then, it was the solution of a puzzle: the Higgs particle is the "last particle" in the minimal standard model. Five years after its discovery, the Higgs boson has allowed to confirm the Standard Model of Particle Physics in a previously unknown sector (Fig. 7.27) and turned into a new tool to explore the manifestations of the SM and to probe the physics landscape beyond it. It should be emphasized that this discovery does not conclude the research in fundamental physics. Some phenomena are not explained by the standard model: neither gravity, nor the presence of dark matter. In addition, as seen in Sect. 7.3.2, the SM has many free parameters: Is this a minimal set, or some of them are calculable?

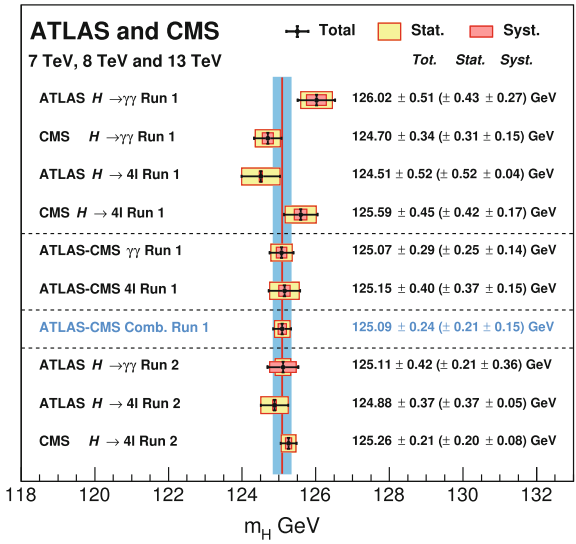

Fig. 7.26 A compilation of decay channels currently measured for the Higgs boson. From C. Patrignani et al. (Particle Data Group), Chin. Phys. C, 40, 100001 (2016) and 2017 update

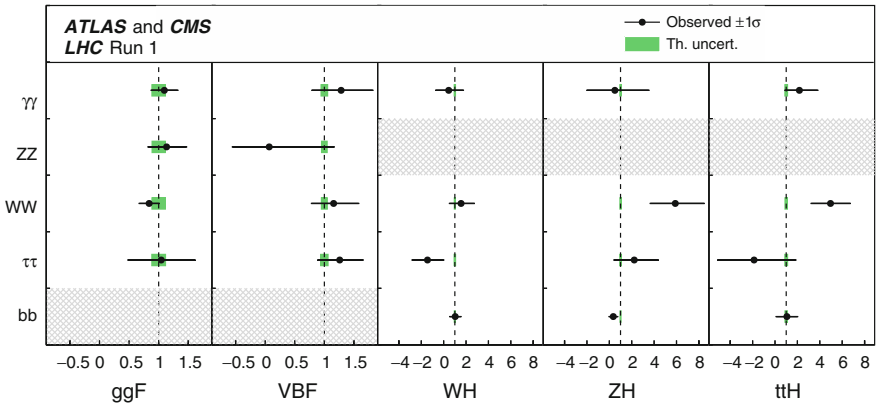

Fig. 7.27 Measurements of the cross section times the branching fraction for the five main production and five main decay modes of the Higgs boson at LHC. The hatched combinations require more data for a meaningful confidence interval to be provided. From C. Patrignani et al. (Particle Data Group), Chin. Phys. C, 40, 100001 (2016) and 2017 update

It is very likely that the SM emerges from a more general (and maybe conceptually simpler) theory.

7.6 Beyond the Minimal SM of Particle Physics; Unification of Forces

We have studied the standard model of particle physics, and we have seen that this model is very successful in describing the behavior of matter at the subatomic level.

Can it be the final theory? This looks very unlikely: the SM seems rather an ad hoc model, and the $SU(3) \otimes SU(2) \otimes U(1)$ looks like a low-energy symmetry which must be part of a bigger picture.

First of all, the standard model looks a bit too complicated to be thought as the fundamental theory. There are many particles, suggesting some higher symmetries (between families, between quarks and leptons, between fermions and bosons) grouping them in supermultiplets. There are many free parameters, as we have seen in Sect. 7.3.2.

Then, it does not describe gravity, which is the interaction driving the evolution of the Universe at large scale.

It does not describe all particles: as we said in Chap. 1, and as we shall discuss in larger detail in the next chapters, we have good reasons to believe that matter in the Universe is dominated by a yet undiscovered kind of particles difficult to accommodate in the standard model, the so-called dark matter.

Last but not least, one of the most intriguing questions is discussed as follows. The fundamental constants have values consistent with conditions for life as we know; sometimes this requires a fine tuning. Take, for example, the difference between the mass of the neutron and the mass of the proton, and the value of the Fermi constant: they have just the values needed for a Sun-like star to develop its life cycle in a few billions of years, which is the time needed for life as we know to develop and evolve. Is this just a coincidence or we miss a global view of the Universe? A minimal explanation is an "anthropic coincidence," which leads to the so-called anthropic principle. The anthropic principle in its weak form can be expressed as "conditions that are observed in the universe must allow the observer to exist" (which sounds more or less like a tautology; note that the conditions are verified "here" and "now"), while one of the strongest forms states that "the Universe must have those properties which allow life to develop within it at some stage in its history." It is clear that on this question the borderline between physics and philosophy is very narrow, but we shall meet concrete predictions about the anthropic principle when shortly introducing the superstring theory. Just to conclude this argument which should deserve a deeper treatment, we cannot avoid the observation that discussions about existence are relevant only for civilizations evolute enough to think of the question—and we are one.

To summarize, many different clues indicate that the standard model is a work in progress and will have to be extended to describe physics at higher energies. Certainly, a new framework will be required close to the Planck scale $\sim 10^{18}$ GeV, where quantum gravitational effects become important. Probably, there is a simplified description of nature at higher energies, with a prospect for the unification of forces.

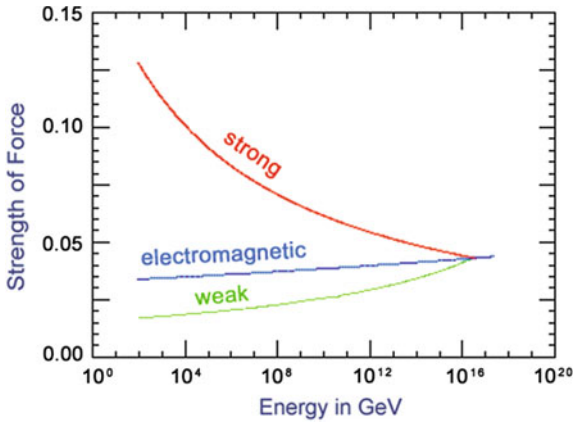

Fig. 7.28 Artistic scheme (qualitative) of the unification of the interaction forces

As we have seen, renormalization entails the idea of coupling parameters "running" with energy. At the energies explored up to now, the "strong" coupling parameter is larger than the electromagnetic constant, which in turn is larger than the weak constant. The strong constant, however, decreases with increasing energy, while the weak and electromagnetic constants increase with energy. It is thus very tempting to conjecture that there will be an energy at which these constant meet—we know already that the weak and electromagnetic constants meet at a large energy scale. The evolution of the couplings with energy could be, qualitatively, shown in Fig. 7.28.

However, if we evolve the coupling "constants" on the basis of the known physics, i.e., of the standard model of particle physics, they will fail to meet at a single point (Fig. 7.31, left). The plot suggests the possibility of a grand unification scale at about 10^{16} eV, but if we want that unification of the relevant forces happens, we must assume that there is new physics beyond the standard model. If also gravity will enter this grand unification scheme, there is no clue of how and at what energy level such unification will happen—but we shall see later that a hint can be formulated.

A unification mechanism requires symmetry groups which include the SM group; it should symmetrize the known particles. Some "grand unification" mechanisms have been proposed; in the following, we shall review the most popular. We stress the fact that no compelling experimental indication of any of these extensions has been found yet–but we are convinced that the SM cannot be the final theory of particle physics.

7.6.1 Grand Unified Theories

The gauge theory of electroweak interactions is unified at high energy under the group $SU_L(2) \otimes U_Y(1)$. This symmetry is spontaneously broken at low energy splitting the electromagnetic and weak interactions. Given the structure of gauge theories in the

standard model, it is tempting to explore the possibility that $\mathrm{SU}_c(3) \otimes \mathrm{SU}_L(2) \otimes \mathrm{U}_Y(1)$ is unified by a larger group G at very large scales of energy such that

$$G \to \mathrm{SU}_c(3) \otimes \mathrm{SU}_L(2) \otimes \mathrm{U}_Y(1)\,.$$

The smallest group including $\mathrm{SU}_c(3) \otimes \mathrm{SU}_L(2) \otimes \mathrm{U}_Y(1)$ is SU(5), proposed by Georgi and Glashow in 1974; this approach, being the first proposed, is called by default the GUT (grand unified theory)—but of course any group including SU(5) can play the game. We shall describe in some detail in this section this "minimal" SU(5) GUT since it is the lowest rank (it has the smallest number of generators) GUT model and provides a good reference point for nonminimal GUTs. However, we should take into account the fact that this simple model has been shown experimentally inadequate, as discussed later.

The symmetry group has 24 generators, which include the extension to rank 5 of the generators of the standard model. A five-dimensional state vector allows to include quarks and leptons in the same vector. As an example, right states will be described all together in a spinor

$$\psi = (d_R, d_G, d_B, e^+, \bar{\nu}_e)\,, \tag{7.104}$$

where the subscript appended to quarks indicates the color.

In addition to the usual transitions involving the exchange of color and the W exchange, gauge bosons corresponding to some of the generators can mediate transitions between quarks and leptons (Fig. 7.29) via the exchange of two new gauge bosons X and Y with electric charges $-4/3$ and $-1/3$, respectively. When extrapolating at masses of order $M_U \sim 10^{15}\,\mathrm{GeV}$, where M_U is the unification mass, all the processes are characterized by a single "grand unified coupling parameter" g_U. At energies $E \ll M_U$, processes involving the exchange of the X and Y bosons are heavily suppressed because of the large masses of these gauge fields, in the same way, as the $W^\pm$ exchange processes are suppressed relative to electromagnetic ones at energies $E \ll M_W$ in the unified electroweak theory.

The Georgi–Glashow GUT is elegant, in the sense that it allows an energy evolution of constants toward a possible unification of forces. In addition, it explains why the quark charges are fractional. We remind that generators of a special unitary group are traceless: the charge operator comes out to be one of the generators of SU(5).

Moreover, with one free parameter only (e.g., assuming that there is actually unification of the interaction strengths, the unification scale, $M_U \simeq 10^{15}\,\mathrm{GeV}$), the

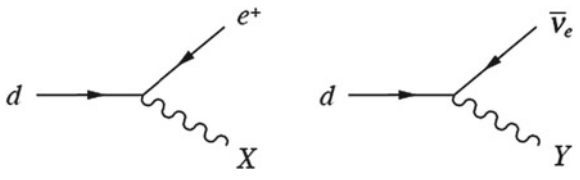

Fig. 7.29 Transitions between quarks and leptons are possible in GUTs

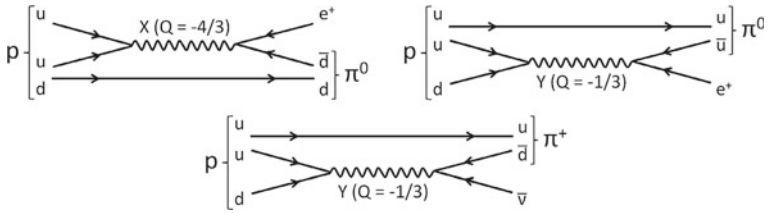

Fig. 7.30 Some mechanisms for proton decay in the SU(5) GUT

theory predicts a value of $\sin^2\theta_W$ close to the one which has been experimentally determined, and the evolution of the $SU(3)_C$, $SU(2)_L$, and $U(1)_Y$ coupling parameters.

Unfortunately, the theory predicts twelve new gauge bosons which are color triplets and flavor doublets as well—they are thus called lepto-quarks. These gauge particles should acquire mass near the unification scale M_U and give rise to the new physics beyond the standard model; among the consequent new phenomena, proton decay has been the object of an intensive and so far unsuccessful experimental search. The $quark \to lepton$ transition can make the proton unstable via the diagrams of Fig. 7.30. Note that the decay channel

$$p \to e^+\pi^0$$

has a clear experimental signature. From the unification mass M_U, one can compute

$$\tau_p \sim 10^{29}\,\text{years}\,.$$

This is a strong prediction: baryonic mass should be unstable.

The experimental lower limit on the proton lifetime,

$$\tau_p > 5.9 \times 10^{33}\,\text{years} \tag{7.105}$$

assuming the branching fractions computed by means of the minimal GUT, rules out the theory. In addition, the LEP precision data indicate that the coupling parameters fail to meet exactly in one point for the current value of $\sin^2\theta_W$, as accurately measured by LEP. Of course one can save GUT by going to "nonminimal" versions, in particular with larger groups and a larger number of Higgs particles; in this way, one loses however simplicity and part of the elegance of the idea—apart possibly for the unification provided by supersymmetry, which we shall examine in next Section.

In his book, "The trouble with physics" (2007), Lee Smolin writes: *"After some twenty-five years, we are still waiting. No protons have decayed. We have been waiting long enough to know that* SU(5) *grand unification is wrong. It's a beautiful idea, but one that nature seems not to have adopted. […] Indeed, it would be hard to underestimate the implications of this negative result.* SU(5) *is the most elegant*

way imaginable of unifying quarks with leptons, and it leads to a codification of the properties of the standard model in simple terms. Even after twenty-five years, I still find it stunning that SU(5) *doesn't work."*

7.6.2 Supersymmetry

The most popular among nonminimal GUTs in particle physics is supersymmetry. Supersymmetry (SUSY) involves a symmetry between fermions and bosons: a SUSY transformation changes a boson into a fermion and vice versa. A supersymmetric theory is invariant under such a transformation. As a result, in a supersymmetric theory, each fermion has a superpartner which is a boson. In the same way, each boson possesses a superpartner which is a fermion. Supersymmetry interconnects different spin particles. This implies an equal number of fermionic and bosonic degrees of freedom.

By convention, the superpartners are denoted by a tilde. Scalar superpartners of fermions are identified by adding an "s" to the name of normal fermions (e.g., the selectron is the partner of the electron), while fermionic superpartners of bosons are identified by adding a "ino" at the end of the name (the photino is the superpartner of the photon). In the Minimal Supersymmetric Standard Model (MSSM), the Higgs sector is enlarged with respect to the SM, having at least two Higgs doublets. The spectrum of the minimal supersymmetric standard model therefore reads as in Table 7.2.

SUSY is clearly an approximate symmetry, otherwise the superpartners of each particle of the standard model would have been found, since they would have the same mass as the normal articles. But as of today, no supersymmetric partner has been observed. For example, the selectron would be relatively easy to produce in $e^- e^+$ accelerators.

Table 7.2 Fundamental particles in the minimal supersymmetric standard model: particles with $R = 1$ (left) and $R = -1$ (right)

Symbol	Spin	Name	Symbol	Spin	Name
e, μ, τ	1/2	Leptons	$\tilde{e}, \tilde{\mu}, \tilde{\tau}$	0	Sleptons
ν_e, ν_μ, ν_τ	1/2	Neutrinos	$\tilde{\nu_e}, \tilde{\nu_\mu}, \tilde{\nu_\tau}$	0	Sneutrinos
d, u, s, c, b, t	1/2	Quarks	$\tilde{d}, \tilde{u}, \tilde{s}, \tilde{c}, \tilde{b}, \tilde{t}$	0	Squarks
g	1	Gluon	$\tilde{g}$	1/2	Gluino
γ	1	Photon	$\tilde{\gamma}$	1/2	Photino
$W^\pm, Z$	1	EW gauge bosons	$\tilde{W^\pm}, \tilde{Z}$	1/2	Wino, zino
H_1, H_2	0	Higgs	$\tilde{H_1}, \tilde{H_2}$	1/2	Higgsinos

Superpartners are distinguished by a new quantum number called R-parity: the particles of the standard model have parity R = 1, and we assign a parity R = −1 to their superpartners. R-parity is a multiplicative number; if it is conserved, when attempting to produce supersymmetric particles from normal particles, they must be produced in pairs. In addition, a supersymmetric particle may disintegrate into lighter particles, but one will have always at least a supersymmetric particle among the products of disintegration.

Always in the hypothesis of R-parity conservation (or small violation), a stable (or stable over cosmological times) lightest supersymmetric particle must exist, which can no longer disintegrate. The nature of the lightest supersymmetric particle (LSP) is a mystery. If it is the residue of all the decays of supersymmetric particles from the beginning of the Universe, one would expect that LSPs are abundant. Since we did not find it, yet, it must be neutral and it does not interact strongly.

The LSP candidates are then the lightest sneutrino and the lightest neutralino χ_0 (four neutralinos are the mass eigenstates coming from the mixtures of the zino and the photino and the neutral higgsinos; in the same way, the mass eigenstates coming from the mixture of the winos and the charged higgsinos are called *charginos*). The LSP is stable or almost stable and difficult to observe because neutral and weakly interacting.

The characteristic signature of the production of a SUSY LSPs would be missing energy in the reaction. For example, if the LSP is a neutralino (which has a "photino" component), the production of a selectron–antiselectron pair in e^+e^- collisions at LEP could be followed by the decay of the two selectrons in final states involving an LSP, the LSPs being invisible to the detection. Since no such events have been observed, a firm limit

$$M_{\mathrm{LSP}} > M_Z/2$$

can be set.

An attractive feature of SUSY is that it naturally provides the unification of forces. SUSY affects the evolution of the coupling parameters, and SUSY particles can effectively contribute to the running of the coupling parameters only for energies above the typical SUSY mass scale (the mass of the LSP). It turns out that within the Minimal Supersymmetric Standard Model (MSSM), i.e., the SUSY model requiring the minimal amount of particles beyond the standard model ones, a perfect unification of interactions can be obtained as shown in Fig. 7.31, right. From the fit requiring unification, one finds preferred values for the break point M_{LSP} and the unification point M_{GUT}:

$$\begin{aligned} M_{\mathrm{LSP}} &= 10^{3.4\pm1.0}\ \mathrm{GeV}, \\ M_{\mathrm{GUT}} &= 10^{15.8\pm0.4}\ \mathrm{GeV}\,. \end{aligned} \tag{7.106}$$

The observation in Fig. 7.31, right, was considered as the first "evidence" for supersymmetry, especially since M_{LSP} and M_{GUT} have "good" values with respect to a number of open problems.

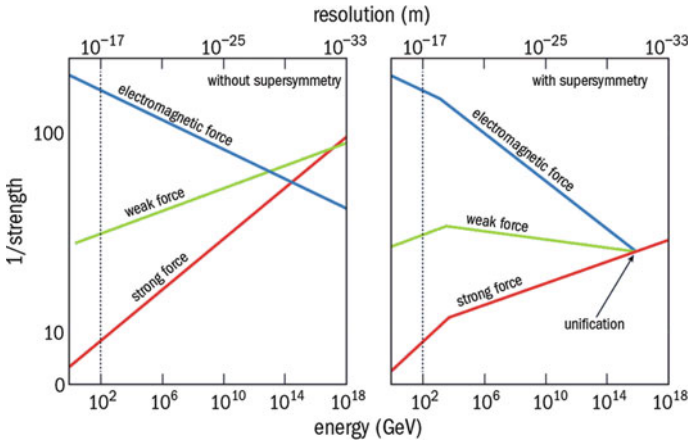

Fig. 7.31 The interaction couplings $\alpha_i = g_i^2/4\pi\hbar c$ fail to meet at a single point when they are extrapolated to high energies in the standard model, as well as in SU(5) GUTs. Minimal SUSY SU(5) model (right) allows the couplings to meet in a point. While there are other ways to accommodate the data, this straightforward, unforced fit is encouraging for the idea of supersymmetric grand unification (Adapted from S. James Gates, Jr., http://live.iop-pp01.agh.sleek.net/2014/09/25/sticking-with-susy/; adapted from Ugo Amaldi, CERN)

In addition, the LSP provides a natural candidate for the yet unobserved component of matter, the so-called dark matter that we introduced in Chap. 1 and we shall further discuss in the next chapter, and which is believed to be the main component of the matter in the Universe. Sneutrino-dominated dark matter is, however, ruled out in the MSSM due to the current limits on the interaction cross section of dark matter particles with ordinary matter. These limits have been provided by direct detection experiments—the sneutrino interacts via Z boson exchange and would have been detected by now if it makes up the dark matter.

Neutralino dark matter is thus the favored possibility. Neutralinos come out in SUSY to be Majorana fermions, i.e., each of them is identical with its antiparticle. Since these particles only interact with the weak vector bosons, they are not directly produced at hadron colliders in copious numbers. A neutralino in a mass consistent with Eq. 7.106 would provide, as we shall see, the required amount of "dark matter" to comply with the standard model of cosmology.

Gravitino dark matter is a possibility in nonminimal supersymmetric models incorporating gravity in which the scale of supersymmetry breaking is low, around 100 TeV. In such models, the gravitino can be very light, of the order of one eV. The gravitino is sometimes called a super-WIMP, as happens with dark matter, because its interaction strength is much weaker than that of other supersymmetric dark matter candidates.

7.6.3 Strings and Extra Dimensions; Superstrings

Gravity could not be turned into a renormalizable field theory up to now. One big problem is that classical gravitational waves carry spin $j = 2$, and present gauge theories in four dimensions are not renormalizable—the quantum loop integrals related to the graviton go to infinity for large momenta, i.e., as distance scales go to zero. Gravity could be, however, renormalizable in a large number of dimensions.

The starting point for string theory is the idea that the point-like elementary particles are just our view of one-dimensional objects called strings (the string scale being smaller than what is measurable by us, i.e., the extra dimension is compactified at our scales).

The analog of a Feynman diagram in string theory is a two-dimensional smooth surface (Fig. 7.32). The loop integrals over such a smooth surface do not meet the zero distance, infinite momentum problems of the integrals over particle loops. In string theory, infinite momentum does not even mean zero distance. Instead, for strings, the relationship between distance and momentum is, roughly,

$$\Delta x \sim \frac{1}{p} + \frac{p}{T_s}$$

where T_s is called the string tension, the fundamental parameter of string theory. The above relation implies a minimum observable length for a quantum string theory of

$$L_{\min} \sim \frac{1}{\sqrt{T_s}} .$$

The zero-distance behavior which is so problematic in quantum field theory becomes irrelevant in string theories, and this makes string theory very attractive as a theory of quantum gravity. The string theory should be the theory for quantum gravity; then this minimum length scale should be at least the size of the Planck length, which is the length scale made by the combination of Newton's constant, the speed of light, and Planck's constant:

$$L_{\min} \sim \sqrt{G} \sim 10^{-35}\,\mathrm{m} . \tag{7.107}$$

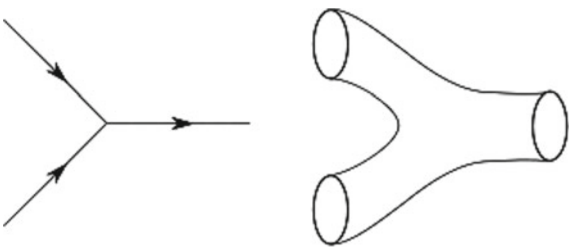

Fig. 7.32 Left: In the Feynman representation, interactions can occur at zero distance—but gravity cannot be renormalized at zero distance. Right: Adding an extra dimension and treating particles as strings solves the problem

One can further generalize the concept on string adding more than one dimension: in this case, we speak more properly of *branes*. In dimension p, these are called $p-$branes.

String theories that include fermionic vibrations, incorporating supersymmetry, are known as superstring theories; several kinds have been described, based on symmetry groups as large as SO(32), but all are now thought to be different limits of a general theory called M-theory. In string theories, spacetime is at least ten-dimensional—it is eleven-dimensional in M-theory.

7.6.3.1 Extra Dimensions Can Reduce the Number of Elementary Particles

An infinite number of N-dimensional particles arises naturally in a $N+1-$ dimensional particle theory. To a N-dimensional observer, the velocity and momentum of a given particle in the hidden extra dimension, which is too small to observe, are invisible. But a particle moving in the $(N+1)$th dimension has a nonzero energy, and the $N-$dimensional observer attributes this energy to the particle's mass. Therefore, for a given particle species living in $N+1$ dimensions, each allowed energy level gives rise to a new elementary particle from the N-dimensional perspective.

A different way of expressing the same concept is that at distance scales larger than the string radius, each oscillation mode of the string gives rise to a different species of particle, with its mass, charge, and other properties determined by the string's dynamics. Particle emission and absorption correspond to the splitting and recombination of string, giving rise to the interactions between particles.

7.6.3.2 Criticism

Although successful, elegant, and theoretically fascinating, string theory is subject to many criticisms as the candidate to the theory of everything (ToE). In particular, it hardly meets the criterion of being falsifiable, since the energies needed to test it can be pushed to values so large that they cannot be reached experimentally. In addition, several versions of the theory are acceptable, and, once one is chosen, it lacks uniqueness of predictions. The vacuum structure of the theory contains an infinite number of distinct meta-stable vacua—some believe that this is a good thing, because it allows a natural anthropic explanation of the observed values of the physical constants.

7.6.4 Compositeness

As we observed in the beginning of this section, one of the characteristics of the standard model which makes it unlikely the final theory is the presence of three

families of quarks and three families of leptons, the second and the third family looking more or less like replicas of the first one.

We were assuming up to now that quarks and leptons are fundamental; we should not forget that in the past, just a century ago, scientists thought that atoms were fundamental—and they could describe approximately their interactions. It was then discovered that atoms are composed of protons, neutrons, and electrons, and protons and neutrons are, in turn, composed of quarks, and some more fundamental interactions are regulating the components. Are these interactions, that the SM of particle physics describes successfully, really fundamental?

We should consider the possibility that quarks and leptons (and maybe also the vector bosons) are composite particles and made of even more elementary constituents. This would change completely our view of nature, as it happened twice in the last century—thanks to relativity and quantum physics. The 12 known elementary particles have their own repeating patterns, suggesting they might not be truly fundamental, in the same way as the patterns on the atomic structure evidenced by Mendeleev suggested that atoms are not fundamental.

The presence of fundamental components of quarks and leptons could reduce the number of elementary particles and the number of free parameters in the SM. A number of physicists have attempted to develop a theory of "pre-quarks," which are called, in general, *preons*.

A minimal number of two different preons inside a quark or a lepton could explain the lightest family of quarks and leptons; the other families could be explained as excitations of the fundamental states. For example, in the so-called *rishon* model, there are two fundamental particles called rishons (which means "primary" in Hebrew); they are spin 1/2 fermions called T ("Third" since it has an electric charge of $e/3$) and V ("Vanishing," since it is electrically neutral). All leptons and all flavors of quarks are ordered triplets of rishons; such triplets have spin 1/2. They are built as follows: TTT = antielectron; VVV = electron neutrino; TTV, TVT, and VTT = three colors of up quarks; TVV, VTV, and VVT = three colors of down antiquarks.

In the rishon model, the baryon number and the lepton number are not individually conserved, while $B - L$ is (demonstrate it); more elaborated models use three preons.

At the mass scale at which preons manifest themselves, interaction cross sections should rise, since new channels are open; we can thus set a lower limit of some 10 TeV to the possible mass of preons, since they have not been found at LHC. The interaction of UHE cosmic rays with the atmosphere reaches some 100 TeV in the center of mass, and thus cosmic rays are the ideal laboratory to observe such pre-constituents, if they exist and if their mass is not too large.

Further Reading

[F7.1] F. Halzen and Martin, "Quarks and Leptons: An Introductory Course in Modern Particle Physics," Wiley 1984. A book at early graduate level providing in a clear way the theories of modern physics in a how-to approach which teaches people how to do calculations.

[F7.2] M. Thomson, "Modern Particle Physics," Cambridge University Press 2013. A recent, pedagogical, and rigorous book covering the main aspects of Particle Physics at advanced undergraduate and early graduate level.
[F7.3] B.R. Martin and G.P. Shaw, "Particle Physics," Wiley 2009. A book at undergraduate level teaching the main concepts with very little calculations.
[F7.4] M. Merk, W. Hulsbergen, I. van Vulpen,"Particle Physics 1," Nikhef 2014. Lecture notes for one semester master course covering in a clear way the basics of electrodynamics, weak interactions, and electroweak unification and in particular symmetry breaking.
[F7.5] J. Romão, 'Particle Physics," 2014, http://porthos.ist.utl.pt/Public/textos/fp.pdf. Lecture notes for one semester master course on theoretical particle physics which is also a very good introduction to quantum field theory.

Exercises

1. *Symmetry breaking introducing a real scalar field.* Consider a simple model where a real scalar field Φ is introduced being the Lagrangian of such field:

$$L = \frac{1}{2}\left(\partial_\mu \Phi\right)^2 - \frac{1}{2}\mu^2\Phi^2 - \frac{1}{4}\lambda\Phi^4$$

   Discuss the particle spectrum originated by small quantum perturbation around the minimum of the potential (vacuum) for the cases $\mu^2 > 0$ and $\mu^2 < 0$. Can such model accommodate a Goldstone boson?
2. *Handling left and right projection operators.* Demonstrate that

$$\left(\frac{1}{2}(1-\gamma_5)\right)\left(\frac{1}{2}(1-\gamma_5)\right) = \left(\frac{1}{2}(1-\gamma_5)\right);$$

$$\left(\frac{1}{2}(1-\gamma_5)\right)\left(\frac{1}{2}(1+\gamma_5)\right) = 0.$$

3. *Fermion mass terms.* Show that the fermion mass term $\mathcal{L}_f = -m_f\bar{\psi}_f\psi_f$ is gauge invariant in QED but not in $\mathrm{SU}(2)_L \otimes \mathrm{U}(1)_Y$.
4. *Mass of the photon.* Show that in the standard model the diagonalization of the $(W3_\mu,\ B_\mu)$ mass matrix ensures the existence of a massless photon.
5. *Fermion couplings.* Verify that choosing the weak hypercharge according to the Gell-Mann Nishijima formula ($Y = 2Q - I_3$) ensures the right couplings of all fermions with the electroweak neutral bosons (Z, Y).
6. $\sin^2\theta_W$. Determine the value of $\sin^2\theta_W$ from the experimental measurements of

   (a) G_F and M_W;
   (b) M_W and M_Z.

7. *W decays.* Compute at leading order the ratio of the probabilities that a $W^\pm$ boson decays into leptons to the probability that it decays into hadrons.

8. *GIM mechanism.* Justify the GIM mechanism, discussed in Sect. 6.3.6.
9. *Fourth family exclusion limit at LEP.* One of the first results of LEP was the exclusion at a level of 5σ of a fourth family of light neutrinos. Estimate the number of hadronic events that had to be detected to establish such a limit taking into account only statistical errors.
10. *Higgs decays into ZZ.* The Higgs boson was first observed in the $H \to \gamma\gamma$ and $H \to ZZ \to 4\, leptons$ decay channels. Compute the branching fraction of $ZZ \to \mu^+\mu^-\mu^+\mu^-$ normalized to $ZZ \to anything$.
11. *Higgs decays into $\gamma\gamma$.* Draw the lowest order Feynman diagrams for the decay of the Higgs boson in $\gamma\gamma$ and discuss why this channel was a golden channel in the discovery of the Higgs boson.